Atomistic/continuum coupling in computational materials science

2003 Modelling Simul. Mater. Sci. Eng. 11 R33

(http://iopscience.iop.org/0965-0393/11/3/201)

INSTITUTE OF PHYSICS PUBLISHING MODELLING AND SIMULATION IN MATERIALS SCIENCE AND ENGINEERING

Modelling Simul. Mater. Sci. Eng. **11** (2003) R33–R68 PII: S0965-0393(03)21576-X

TOPICAL REVIEW

Atomistic/continuum coupling in computational materials science

W A Curtin[1] **and Ronald E Miller**[2]

[1] Division of Engineering, Brown University, Providence, RI 02912, USA
[2] Department of Mechanical and Aerospace Engineering, Carleton University, Ottawa, ON, Canada K1S 5B6

Received 28 January 2003, in final form 27 March 2003
Published 24 April 2003
Online at stacks.iop.org/MSMSE/11/R33

Abstract

Important advances in multi-scale computer simulation techniques for computational materials science have been made in the last decade as scientists and engineers strive to imbue continuum-based models with more-realistic details at quantum and atomistic scales. One major class of multi-scale models directly couples a region described with full atomistic detail to a surrounding region modelled using continuum concepts and finite element methods. Here, the development of such coupled atomistic/continuum models is reviewed within a single coherent framework with the aim of providing both non-specialists and specialists with insight into the key ideas, features, differences and advantages of prevailing models. Some applications and very recent advances are noted, and important challenges for extending these models to their fullest potential are discussed.

1. Introduction

The mechanical deformation and failure of many engineering materials are inherently multi-scale phenomena in that the observed macroscopic material behaviour is governed by processes that occur on many different length and timescales. In this review, we will be concerned with bridging length scales; bridging timescales from the picosecond times of atomistic vibrations to the micro-, milli- and larger times scales of various defect motions is an equally difficulty but fundamentally different matter. At the smallest length scale of Angstroms, quantum mechanical interactions and atomic structure provide an underlying framework for the elastic deformation of materials and, more importantly, for the formation of a wide variety of defects in otherwise crystalline solids. Although nanometre-scale defects such as vacancies, impurities, dislocations, voids, crack tips and grain boundaries correspond to specific atomic configurations involving many atoms, they can also be viewed as individual mechanical entities with specific properties. The deformation fields associated with these defects leads to defect

interactions at even larger scales (from nanometres to many microns) such as dislocation patterning, crack tip shielding by dislocations and solute hardening. Often, these phenomena are controlled by long-range fields that do not require a fully atomistic description of the defect core. Macroscopic behaviour is a manifestation of the interaction and organization of this myriad collection of possible defects within a polycrystalline microstructure that may range in size from microns to millimetres.

There is an intimate coupling between the disparate length scales, as the long-range defect stress fields can cause the nucleation of new defects at the atomic-scale or drive the motion of existing defects. Although theories at higher length scales attempt to subjugate the smaller scale phenomena into 'effective' properties or 'constitutive rules,' macroscopic phenomena of prime interest in material applications such as fracture and fatigue degradation, ultimately depend on the details of smaller scale phenomena. On the other hand, full atomistic description of individual defects alone does not provide for the determination of macroscopic behaviour, since the higher scale defect interactions collectively operate to drive large-scale behaviour. Realistic methods and approaches for effecting the coupling of length scales (CLS) is a great challenge for computer simulations.

Fully atomistic simulation of most collective defect processes, such as fracture, is simply not feasible. Current state-of-the-art, massively parallel supercomputer simulations can handle about 10^9 atoms using a simple empirical potential, amounting to a volume of less than 1 cubic micron. Even with substantial future increases in computational power, attaining the scale needed for typical polycrystals (at least 10^6 cubic microns) is unlikely. Atomistics must be used in conjunction with larger scale methods through multi-scale modelling techniques.

There are two conceptually different approaches that have been taken to address multi-scale modelling problems. The first approach involves the passing of critical information obtained from atomic-scale models to mesoscale or continuum models. This approach has been used for decades in one guise or another. At the simplest level, elastic constants, thermal expansion coefficients and other properties of defect-free crystals can be extracted from atomistic models as constitutive material property input in continuum models. Information about dislocation slip systems and other dislocation properties have been used in the formulation of crystal plasticity models. More recently, workers have performed atomistic or quantum level calculations of material separation to supply cohesive zone parameters for continuum models of fracture nucleation and propagation using cohesive zone models [1, 2]. Mesoscale simulations of plasticity, as modelled by discrete dislocations, take as input dislocation information such as the Burgers vector, Peierls stress, strength of Frank-Read dislocation sources and dislocation mobility, that can be derived from careful atomistic studies of single defects [3–5]. Problems involving diffusion and/or chemical reactions have been tackled by using atomistic simulations to obtain a broad spectrum of the relevant rate phenomena which then becomes the database for kinetic Monte Carlo simulations of larger scale system evolution [6].

The approach of 'passing' information from smaller to larger scale models is powerful in that no direct coupling of computational methods at different scales is needed. However, such methods can be limited because the small scale phenomena are parametrized via studies of simple defect geometries that may not capture the full complexity of deformation that would emerge from a hypothetical, fully atomistic treatment. Therefore, co-incident with the rise of the information-passing methods has been the development of explicitly coupled models where full atomistic detail is retained in one or a few critical regions of the material while mesoscale or continuum models are employed to describe deformation in regions of the material that are more remote from the complex atomistic behaviour. Such approaches, which will be the focus of this article, can be appropriate and useful when important atomic-scale phenomena are relatively localized in space, such as at a crack tip, grain boundary,

or nanoindenter. Models that allow for the simultaneous, mechanically-coupled simulation of an atomistic and a continuum region are truly multi-scale: atomistic phenomena are properly described where necessary while continuum mechanics approaches in surrounding regions are used to significantly reduce the computational burden without compromising accuracy.

Coupled methods are not entirely new; their origins lie in work of the 1970s [7–9] that used continuum elasticity to provide realistic boundary conditions for atomistic regions that, by current computational standards, were tiny (e.g. Sinclair [9] reports crack tip studies using 924 atoms). From the beginning, there were signs that the coupling of atomistics and continua would not be simple; Gehlen reported in [8] that the original conclusions drawn in [7] were incorrect because of the effect of isotropic, rather than anisotropic, treatment of the continuum region. The work of Sinclair [9] provided a prelude to the fully numerical treatment of the continuum region that was to follow in later work: Sinclair's analytical treatment of the continuum region made use of a weighted superposition of equilibrium solutions that allowed the boundary conditions to be modified during the energy minimization of the atomistic region. By the early 1980s, the continuum region was being modelled explicitly using the finite element (FE) method [10–12]. In fact, all of the current coupled methods to be discussed here continue to use FE in the continuum region despite the existence of other numerical continuum approaches. This is likely due to the natural way in which a discrete FE mesh with displacement degrees of freedom can, when refined to atomic dimensions, be made to correspond with an underlying set of atomic positions (as will be evident from what follows).

A number of reviews of multi-scale methods have been written in recent years, with varying purpose and level of detail (see, e.g. [13–18]). The purpose of this review is to compare and contrast the details of several models developed for molecular statics or dynamics problems so as to provide users of these methods with a better understanding of the relationships among them and to offer the newcomer a clear picture of the physics, complexities and capabilities of these computational approaches. This review is thus organized as follows. In the next section, some basic concepts in atomistic and continuum FE methods are introduced. In section 3, the generic atomic/continuum coupling problem is described and the various methods used to date to handle this coupling are discussed. A simple one-dimensional model is then introduced and used to elucidate some of the fundamental artefacts associated with an atomistic/continuum boundary. Section 4 addresses recent extensions of the static zero temperature models to finite temperatures and dynamics, while section 5 presents a sampling of the types of problems that have been studied using the various methods. Some concluding remarks are provided in section 6.

2. Background Basics

At the heart of the computational methods related to atomistic/continuum coupling is a determination of the total potential energy of a system as a function of the degrees of freedom (e.g. atom or FE nodal positions). Static equilibrium at zero temperature follows by minimizing the total energy or, equivalently, finding the zero-force positions for every degree of freedom (dof) where the force on a dof is the derivative of the total energy with respect to the dof coordinate. In dynamic simulations, the force is used in Newton's second law to evolve the system in time. We thus begin with a brief primer on the energetics of atomistic and continuum systems. For readers unfamiliar with either of these methods, we suggest the review by Carlsson [19] for atomistic modelling and any of a number of introductory FE textbooks such as those by Hughes [20] or Zienkiewicz [21].

2.1. Atomistics

Energetics at the atomic-scale is governed by quantum mechanics. Quantum mechanical total energy calculations provide the energy as a function of the collective nuclear coordinates, which are also the degrees of freedom in an atomic-scale calculation. The energy functional is minimized with respect to the electronic degrees of freedom for fixed nuclear coordinates. The force on an individual nucleus can then be obtained by taking the derivative of the total energy with respect to the desired nuclear coordinate. Because the electronic degrees of freedom have been condensed out through minimization, the electronic wavefunctions or density can be held fixed during the differentiation, so that the so-called Hellman–Feynmann force on the nucleus can be obtained relatively easily. The review article by Payne *et al* [22] addresses many of the details and subtleties of quantum energy calculations and associated molecular dynamics. There has only been one effort to date that uses quantum mechanics to obtain energies and forces on individual atoms in a coupled method [18,23], however, and so here we will emphasize the much more widespread methods that employ effective classical interatomic potentials. An important difference, aside from the approximate and semi-empirical nature of the interatomic potentials described below, is that the quantum energy cannot be partitioned into energies on a per-atom basis, while the classical energies can be so partitioned. More precisely, the total atomic energy, E^a, when obtained from classical potentials, admits the form

$$E^a = \sum_i E_i, \tag{1}$$

where E_i is the energy of the ith atom. The quantum mechanical description of this energy cannot be divided unambigously between the atoms. Some of the coupled methods described below rely on the classical partitioning on a per-atom or per-bond basis, and hence they cannot immediately be extended to use quantum energetics.

Classical interatomic potentials are most widely used in either the embedded-atom method (EAM) [24,25] or Stillinger–Weber (SW) [26] type framework. In both, the energy is expressed as a sum of individual atom energies. The EAM constitutive law for an atom energy involves an embedding energy associated with the cost of embedding the atom into the sea of electrons of the surrounding atoms, and is inherently non-local with many-body interactions included implicitly. Specifically, the EAM energy of an atom i is given by

$$E_i = F_i(\bar{\rho}_i) + \frac{1}{2}\sum_{j\neq i} V_{ij}(r_{ij}), \tag{2}$$

where F_i is an electron-density dependent embedding energy, V_{ij} is a pair potential between atom i and its neighbour j and r_{ij} is the interatomic distance. The electron density at atom i, $\bar{\rho}_i$, is the superposition of density contributions from each of the neighbours, ρ_j:

$$\bar{\rho}_i = \sum_{j\neq i} \rho_j(r_{ij}). \tag{3}$$

The SW-type energies involve explict two- and three-body site interaction terms, the latter accounting for directional bonding in covalent materials. The energy of an atom i in the SW formulation is then

$$E_i = \frac{1}{2}\sum_{j\neq i} V_{ij}(r_{ij}) + \frac{1}{6}\sum_{j\neq i}\sum_{k\neq(i,j)} V^{(3)}_{ijk}(\boldsymbol{r}_{ij}, \boldsymbol{r}_{ik}), \tag{4}$$

where $V^{(3)}_{ijk}$ is the three-body potential and $\boldsymbol{r}_{ij}$ is the vector from atom i to neighbour atom j. In both the EAM and the SW frameworks, the exact details of the functions ρ_j, F_i, V_{ij} and $V^{(3)}_{ijk}$ are defined with a range of parameters. These parameters are then adjusted to produce a best-fit to various properties, experimentally measured and/or calculated via first-principles quantum mechanics [27, 28], for a given material.

An important aspect of interatomic potentials that adequately represent real materials is that the interaction energies extend beyond near-neighbour atoms. The potentials are thus non-local, in theory extending over all space but in practical implementations extending over a range R_{cut} on the order of the first few neighbour distances.

Other formulations for interatomic potentials exist, such as the modified EAM [29] and the Tersoff–Brenner [30, 31] potentials. These may be more accurate and useful for certain classes of materials but are based upon ideas similar to those of either the EAM and SW. A recent development is the so-called 'Bond-order Potential' approach [32, 33] that stems from formal quantum mechanical arguments associated with the bonding of valence electrons, and can represent some features of atomic interactions accurately without extensive fitting. These potentials are still augmented by an additional atom-pair interaction to provide the short-range atomic repulsion, however, and thus some fitting to material properties remains.

Given the atomic potentials as a function of the atomic coordinates $\{\boldsymbol{r}_1 \cdots \boldsymbol{r}_N\}$, the total potential energy is the simple sum of equation (1). Forces on each atom are obtained as

$$\boldsymbol{f}_i = -\frac{\partial E^a(\{\boldsymbol{r}_1 \cdots \boldsymbol{r}_N\})}{\partial \boldsymbol{r}_i} \tag{5}$$

in the absence of externally applied forces. The availability of both the total energy and the forces permits application of the conjugate-gradient method to efficiently minimize the total energy to obtain the static, zero-temperature equilibrium atomic configuration as a function of applied forces and imposed displacements on specific atoms.

Note that in atomistic calculations, there is no direct consideration of the continuum concepts of strain or displacement. One simply follows the motion of individual atoms without reference to their original positions. In fact, the 'deformations' that can occur in atomistic simulations explicitly violate many assumptions about the continuity of deformations, the invertibility of deformation maps and other tenets of continuum mechanics.

2.2. Continuum concepts and their relation to atomistics

Continuum mechanics tacitly assumes that a strain energy density functional W exists for a material. Hence, the energy in an incremental volume $\mathrm{d}\boldsymbol{V}$ around point $\boldsymbol{X}$ is $W(\boldsymbol{X})\,\mathrm{d}\boldsymbol{V}$. The origin of this energy functional and its dependence on the strain of the material is input to the continuum model. The overall potential energy of the material is then an integral over the volume Ω of the body,

$$E^c = \int_\Omega W(\boldsymbol{X})\,\mathrm{d}\boldsymbol{V}. \tag{6}$$

Because the predominant assumption used in coupled methods is that the continuum regions do not contain any large deformations or inelastic phenomena, it is common to employ linear elasticity in this region so that the energy density is simply

$$W_{\text{lin}}(\boldsymbol{X}) = \tfrac{1}{2}[\boldsymbol{C} \cdot \boldsymbol{\epsilon}(\boldsymbol{X})] : \boldsymbol{\epsilon}(\boldsymbol{X}), \tag{7}$$

where $\boldsymbol{C}$ is the fourth-order tensor of elastic constants of the material, $\boldsymbol{\epsilon}(\boldsymbol{X})$ is the strain tensor evaluated at the point $\boldsymbol{X}$, and: implies the fully-contracted inner product. Typically, the constants $\boldsymbol{C}$ are obtained from experiments or first-principles calculations.

A small digression on the kinematics of continuum deformations is useful at this point. Starting from the stress-free reference state of the undeformed perfect crystal, a deformed state can be characterized by a deformation gradient $\boldsymbol{F}(\boldsymbol{X})$. Imagine a point $\boldsymbol{X}$ in the undeformed material that is moved, by some applied forces or imposed displacements on the body, to the point $\boldsymbol{x}$. The displacement referenced to the original state of the material is $\boldsymbol{u}(\boldsymbol{X}) = \boldsymbol{x} - \boldsymbol{X}$. The deformation gradient $\boldsymbol{F}(\boldsymbol{X})$ is a second-rank tensor that maps an infinitesimal vector $\mathrm{d}\boldsymbol{X}$ at point $\boldsymbol{X}$ in the reference state to the infinitesimal vector $\mathrm{d}\boldsymbol{x}$ at $\boldsymbol{x}$ in the deformed state. The difference $\mathrm{d}\boldsymbol{x} - \mathrm{d}\boldsymbol{X}$ describes the local deformation (stretching and rotating) referenced to the original point $\boldsymbol{X}$ and the deformation gradient is simply

$$\boldsymbol{F}(\boldsymbol{X}) = \frac{\mathrm{d}\boldsymbol{x}}{\mathrm{d}\boldsymbol{X}} = \boldsymbol{I} + \nabla \boldsymbol{u}(\boldsymbol{X}), \tag{8}$$

where ∇ is the gradient with reference to $\boldsymbol{X}$. The strain referenced to the point $\boldsymbol{X}$ is then quantified by the Lagrangian strain

$$\boldsymbol{E} = \tfrac{1}{2}(\boldsymbol{F}^{\mathrm{T}}\boldsymbol{F} - \boldsymbol{I}), \tag{9}$$

which in the limit of infinitesimal deformations (small strains) reduces to the usual small strain tensor $\boldsymbol{\epsilon} = [\nabla \boldsymbol{u} + (\nabla \boldsymbol{u})^T]/2$.

To solve for the equilibrium strain field associated with some applied forces and displacements in the body, the energy E^c must be minimized. The FE method is a standard procedure for approximately carrying through the minimization. The idea in FE is to introduce a set of points $\boldsymbol{X}_j$ (the nodes j) at which the displacements $\boldsymbol{U}_j = \boldsymbol{u}(\boldsymbol{X}_j)$, will be calculated. The displacements at locations away from the nodes are assumed to be given by an interpolation of the nodal displacements to the desired location using predetermined interpolation or shape functions. Elements are formed by defining polyhedral regions with the nodes at vertices, such that the entire space is tesselated by elements. It is common that the shape functions used in the FE method have what is referred to as compact support, meaning that the functions associated with a node j are non-zero only in elements immediately adjacent to j. In this way, the displacement of a point within an element depends only on the displacements of the nodes corresponding to the vertices of the element. By restricting the degrees of freedom to the displacements of the nodes, the FE method imposes a kinematic constraint on the deformation of the material. This formulation can be succinctly described as follows.

The total energy of the continuum region is the integral over the body of the strain energy density, which can be written as the sum over the elements μ as

$$E^c = \int_\Omega W \,\mathrm{d}\boldsymbol{V} = \sum_{\mu}^{N_e} E_\mu, \tag{10}$$

$$E_\mu = \int_{\Omega_\mu} W(\boldsymbol{X}) \,\mathrm{d}\boldsymbol{V}, \tag{11}$$

$$W(\boldsymbol{X}) = W(\boldsymbol{F}(\boldsymbol{X})), \tag{12}$$

where N_e is the number of elements in the region, Ω_μ is the volume of element μ and the strain energy density, W, depends on the deformation, in general, through $\boldsymbol{F}$. The integral over each element is efficiently handled using Gaussian quadrature. The convention adopted above and for the remainder of this paper is to use Latin subscripts to refer to atom or node numbers and Greek subscripts to refer to element numbers. We have somewhat restricted the generality of the formulation at this point by assuming a hyperelastic material (i.e. W is a function only of $\boldsymbol{F}$).

The discretization and interpolation of the displacement field allows for the computation of the displacements within the elements by

$$\boldsymbol{u}(\boldsymbol{X}) = \sum_{j=1}^{N} \boldsymbol{U}_j S_j(\boldsymbol{X}), \tag{13}$$

$$\boldsymbol{F}(\boldsymbol{X}) = \boldsymbol{I} + \sum_{j=1}^{N} \boldsymbol{U}_j \otimes \nabla S_j(\boldsymbol{X}), \tag{14}$$

where N is the number of nodes in the region, $\otimes$ is the tensor product and S_j is the shape function associated with node j.

For defect-free perfect crystalline material, the functional $W(\boldsymbol{X})$ can be connected directly to material properties as follows. The locality of $W(\boldsymbol{X})$ implies that the strain energy density at $\boldsymbol{X}$ is equal to the strain energy per unit volume of an infinite perfect crystal deformed according to a homogeneous deformation gradient equal to $\boldsymbol{F}(\boldsymbol{X})$. The strain energy per unit volume of an infinite crystal can easily be calculated, by interatomic potentials or first-principles, as the energy of a single unit cell of a material under the homogeneous deformation $\boldsymbol{F}(\boldsymbol{X})$ divided by the unit cell volume. Since the fundamental quantity of continuum deformation is the deformation gradient $\boldsymbol{F}(\boldsymbol{X})$, this atomistic energy calculation is easily performed using the Cauchy–Born rule [34–36], first elucidated within the context of coupled methods by Tadmor *et al* [37]. Specifically, given a deformation gradient $\boldsymbol{F}$, the deformed unit cell is generated by mapping the primitive Bravais lattice vectors of the undeformed crystalline structure $(\boldsymbol{A}_i, i = 1, \ldots, 3)$ into the deformed vectors $\boldsymbol{a}_i = \boldsymbol{F}\boldsymbol{A}_i$. The $\boldsymbol{a}_i$ specify the new locations of the lattice sites in the crystal, such that any lattice site is obtained from a set of 3 integers (l, m, n) as

$$\boldsymbol{R} = l\boldsymbol{A}_1 + m\boldsymbol{A}_2 + n\boldsymbol{A}_3 \tag{15}$$

in the undeformed lattice and

$$\boldsymbol{r} = l\boldsymbol{a}_1 + m\boldsymbol{a}_2 + n\boldsymbol{a}_3 \tag{16}$$

after the deformation. For materials with a simple Bravais lattice, where there is one atom per unit cell which is typically taken to sit at the lattice site, this procedure is unambiguous in creating a deformed unit cell. For complex crystals, where there is more than one atom associated with each lattice site, the atom locations are described by basis vectors $\boldsymbol{B}_k$, $(k = 1, \ldots, n)$ relative to the lattice site. The actual undeformed atom positions are $\boldsymbol{R} + \boldsymbol{B}_k$, $k = 1, \ldots, n$. The Cauchy–Born rule strictly applied to such systems then dictates that the deformed atom locations are

$$\boldsymbol{r}_k = l\boldsymbol{a}_1 + m\boldsymbol{a}_2 + n\boldsymbol{a}_3 + \boldsymbol{b}_k, \tag{17}$$

where

$$\boldsymbol{b}_k = \boldsymbol{F}\boldsymbol{B}_k \tag{18}$$

and the energy density is then

$$W(\boldsymbol{F}(\boldsymbol{X})) = \frac{E_a[\boldsymbol{F}(\boldsymbol{X})]}{\Omega_0}, \tag{19}$$

where Ω_0 is the volume of a primitive unit cell of the material.

The Cauchy–Born rule is similar to the FE assumption in that atomic degrees of freedom internal to the unit cell are kinematically slaved to the positions of the Bravais lattice sites. This prescription does not permit relaxation of the basis atoms within the unit cell so that the energy calculated using the Cauchy–Born rule applied to all atoms is accurate only in the limit of small deformations. To obtain exact results, it is necessary to impose the Cauchy–Born

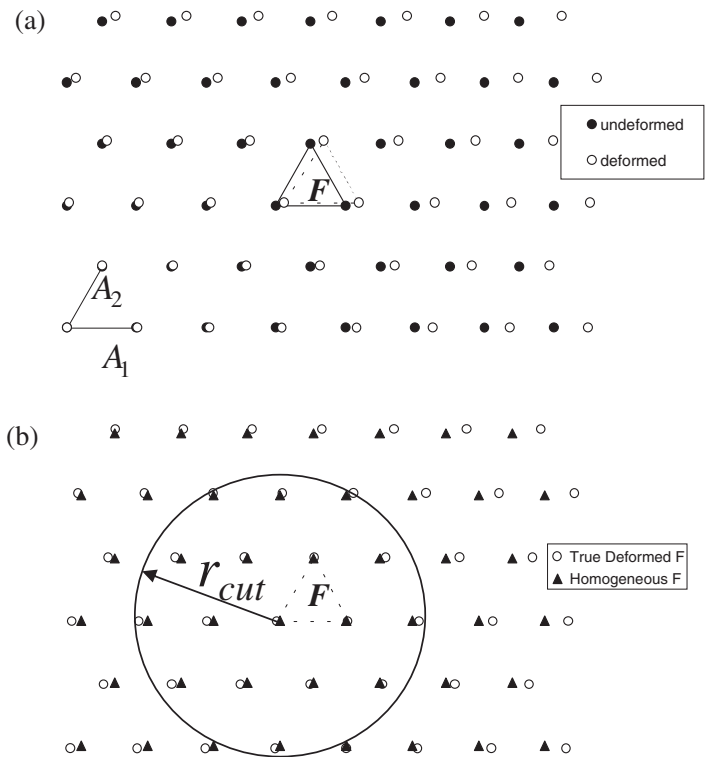

Figure 1. A reference lattice experiences some inhomogeneous deformation as shown in (*a*), leading to the deformation gradient $\boldsymbol{F}$ in one element (at the Gauss point $\boldsymbol{X}_g$ not shown). The local approximation assumes that the entire lattice deforms according to the uniform deformation gradient $\boldsymbol{F}$, leading to the approximate deformed state shown in (*b*).

rule on the atoms occupying the lattice sites only ($k = 1$) and then minimize the energy with respect to the 'internal' degrees of freedom $\boldsymbol{b}_k$ ($k = 2, \ldots, n$) for the other basis atoms.

The locality of the strain energy density functional $W(\boldsymbol{X})$ is a crucial assumption when attempting to construct coupled methods. As noted above, the true atomistic energy is non-local. Hence, when the gradient of the deformation gradient, $\nabla \boldsymbol{F}$, is large such that the deformation gradient changes appreciably over scales approaching the atomic spacing, the non-locality plays an important role and the local strain energy density functional simply cannot capture this non-locality. When $W(\boldsymbol{X})$ is calculated in the continuum model, it does include the non-locality of the atomic interactions but it does so by assuming a homogeneous deformation around any given element rather than considering the true inhomogeneous deformation. To make this important point concrete, consider a two-dimensional lattice of atoms in some inhomogeneously deformed state, as shown in figure 1(*a*). Let a continuum approximation for the energy of this system be generated by considering each and every atom as a node in a mesh of the continuum region, so that the kinematics of the continuum model is exact. Now consider the continuum energy of one particular triangular element for which the deformation gradient at the Gauss point $\boldsymbol{X}_g$ is $\boldsymbol{F}$. The continuum energy for this element is calculated as if the deformation $\boldsymbol{F}$ is applied everywhere throughout the material. Applying $\boldsymbol{F}$ to every node in the undeformed lattice leads to the atomic positions shown in figure 1(*b*) that are overlayed with the actual deformed atomic positions. The continuum strain energy density corresponds

to an atomistic calculation of the energy for this approximate set of atomic positions. Thus, the continuum energy accounts for the non-local/finite-range of the interatomic potentials, but with an approximation to the atomic positions. The difference between the true atomic positions and those assumed in the continuum calculation of the strain energy of a particular element is associated with the gradient of $\boldsymbol{F}(\boldsymbol{X})$. When the deformation gradient is sufficiently smooth over the scale of the non-locality of the interatomic interactions (i.e. $|\nabla \boldsymbol{F}\boldsymbol{A}_1| \ll 1$), the FE approximation to the element energy is accurate. Note that, as evident in figure 1(*b*), nodes further from the element of interest are in positions increasingly different than the actual atom positions, but since the interatomic interactions are generally relatively short-range these poor estimates of the distant atom positions do not affect the energy calculation. However, for systems with truly long-range potentials (e.g. Coulomb potentials), these differences can become important in computing the energy.

To establish mechanical equilibrium, the energy described above is minimized with respect to the nodal degrees of freedom. It is thus useful to identify the consequences of the local approximation of $W(\boldsymbol{X})$ on the nodal forces. The force on node i is calculated as $-\partial E^c/\partial \boldsymbol{U}_i$, and thus corresponds to the energy change upon 'wiggling' node $\boldsymbol{U}_i$ by an infinitesimal amount. In the FE, a change in the displacement of node i causes a change in the deformation gradients $\boldsymbol{F}$ of all of the elements in which node i is contained and hence a change in the total energy due only to changes in these same elements,

$$\frac{\partial E^c}{\partial \boldsymbol{U}_i} = \sum_{\mu=1}^{n_e} \frac{\partial E^c_\mu}{\partial \boldsymbol{U}_i}, \tag{20}$$

where the sum is over the n_e elements connected to node i. The energies associated with elements not connected to node i do not change. In contrast, when one atom is displaced in an atomistic simulation, all atoms within the range R_{cut} of the potential experience an energy change. Within an atomistic formulation in which the energy can be decomposed according to equation (1), the force on atom i is

$$\frac{\partial E^a}{\partial \boldsymbol{r}_i} = \sum_{(j, r_{ij} < R_{\text{cut}})} \frac{\partial E_j}{\partial \boldsymbol{r}_i}, \tag{21}$$

where the sum is over the energy of each atom within R_{cut} of the atom i. Thus, the volume of material governing the calculation of the forces in the FE approximation depends on the mesh, and differs from the atomic forces. This can give rise to various artefacts in both static and dynamic situations, as will be discussed further below.

3. Coupled atomistic/continuum methods

In this section, we discuss the details of several coupled methods, with a goal of trying to use a common language and notation for the purposes of comparison. One important point that will emerge is that some of these methods have a well-defined energy functional that approximates the potential energy due to the deformation for the entire model, i.e. the energy of both the atomistic and continuum regions combined. Between methods with energy functionals, it is possible to make a direct comparison of the energy functionals to see the similarities between the methods. In effect, these methods achieve the coupling of the atomistic and continuum at the level of the energy functional. However, several of the methods that will be presented deliberately do not incorporate a unified energy functional. In some cases, separate energy descriptions for each domain are used, with the coupling of the atomistic and the continuum achieved through a solution procedure that effectively incorporates each domain

into the boundary conditions of the other. As we will illustrate below, the advantage to this latter approach is an elimination of spurious relaxations in the transition region between the atomistic and continuum, but at the possible expense of somewhat slower convergence rates.

3.1. The transition region

In coupled methods, the idea is to use a fully atomistic description in one region of material and a continuum description in other regions. The detailed treatment of the material in the 'transition region' or boundary between the atomistic and continuum regions is a critical aspect of such an approach. Nearly all of the existing methods have a well-defined transition region in which some approximation is made. An approximation is necessary due to the fundamental incompatability of the non-local atomistic description and the local continuum description, as highlighted above. Variations among the existing coupling methods are a result of differences in desired application of the method, intuitive identification of important physical phenomena, and issues related to practical, computationally-efficient implementation. A unified and formal theory of the transition region that allows quantifiable error bounds to be established does not yet exist. Here, the details of the transition region employed in the quasicontinuum (QC) method of [37,38], the CLS method[3] of [39], the FEAt method of [40], the fully non-local QC (QC-FNL) method of [41], and the CADD method of [42] will be discussed and compared. As a starting point, a generic description of this transition region is presented, followed by a discussion of the potential energy functionals employed in each of these models.

The generic transition region is shown schematically in figure 2. On one side of the transition region is the atomistic region in which every atom is explicitly represented and treated using interatomic potentials. On the other side, there is a FE mesh with its associated nodes in which, typically, the nodes sit on atomic lattice sites although not all atom sites are nodal positions. At the interface between the FE nodes and the atoms there is a one-to-one correspondence between atoms and nodes on the FE mesh. Moving away from the interface on the continuum side, the FE nodes become increasingly sparse and the corresponding elements become larger so as to always completely fill the physical space. Finally, there is a 'pad' region where pseudoatoms exist on the continuum side of the interface and overlap physical space with the FEs. Some of the 'pad' atoms coincide with the FE nodes while others lie within the elements. The pad of pseudoatoms is a device used to help account for the non-local interactions between atoms so that real atoms at and near the interface see a full complement of neighbours. Without the pad atoms, a non-physical surface energy is introduced into the problem. As we shall discuss, the use of the pad atoms, and the prescription for determining their positions differs among the different methods. At this stage of generality, the pad is represented as a set of atoms that are degrees of freedom that can, in principle, be separate from the nodes in the FE mesh.

In the following discussion, atoms in the true atomistic region, atoms on the interface, and pseudoatoms in the pad will be denoted by the subscripts 'A', 'I' and 'P' respectively. Note that the terminology and description of the transition is chosen so that the various methods can be described within a common framework.

3.2. The QC method

The QC method [37, 43, 38] has been used to study a variety of fundamental aspects of deformation in crystalline solids, including fracture [44–47], grain boundary structure and

[3] Note that the focus here is only on the coupling between that atomistic and the continuum in the CLS method, not on the coupling between the tight-binding (TB) and semi-empirical atomistic regions.

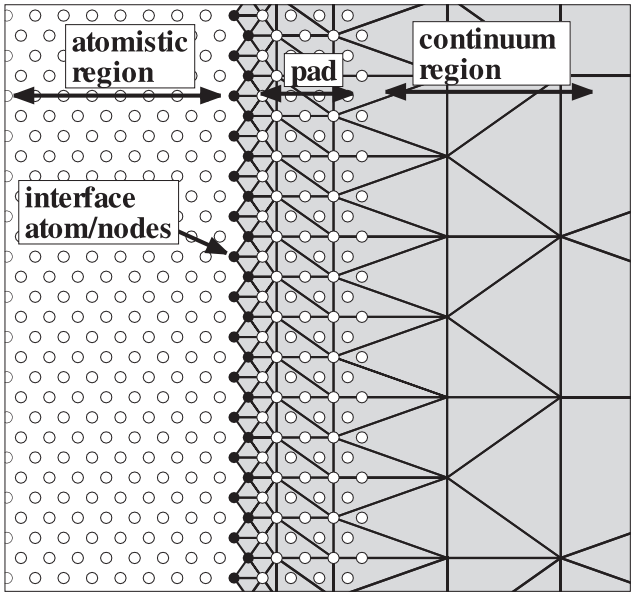

Figure 2. The generic form of the atomistic/continuum transition region for the methods discussed herein. Filled atoms are the atoms right on the interface, which coincide with a set of FE nodes in the continuum. The 'pad' atoms serve only as a neighbour environment to the atoms in the atomistic and interface regions. For many of the methods, some or all of the 'pad' atoms are chosen to coincide with nodes in the mesh.

deformation [38, 43], nano-indentation [48–53] and three-dimensional dislocation junctions [54–57]. The original implementation was for two-dimensional static equilibrium problems, but the method has been naturally extended to three-dimensional in both [41, 54] and to finite temperatures by [58]. A recent review of the QC method can be found in [59].

The QC method defines two types of atoms, 'local representative atoms' and 'non-local representative atoms', rather than identifying atomistic and continuum regions. In practice, however, the regions containing non-local representative atoms are essentially equivalent to the fully atomistic regions of other methods. Similarly, a local representative atom is co-incident with either a continuum FE node or an atomic position near a Gauss point used to define the energy of the continuum element. The language of non-local and local clearly associates the non-local atoms with 'real' atoms and the local atoms with the local FE region.

The transition region between non-local and local representative atoms in the QC model is depicted in figure 3. The interface atoms are included in the atomistic energy but are also FE nodes of the continuum. The pad atom positions $\boldsymbol{r}_P$ are dictated by interpolation from the FE nodal positions. The pad atom energies are not included but the energies of the real and interface atoms include their interactions with the pad atoms. To avoid overcounting of the energy of the interface atoms/nodes, the energies of the continuum elements adjacent to the interface (i.e. elements that have nodes corresponding to the interface atoms as shown in grey in the figure) are weighted differently in the total potential energy sum. The total potential energy of the QC model is then obtained by summing the energies of all atoms in the atomistic region and at the interface and all elements in the continuum domain as

$$E_{\mathrm{QC}} = \sum_{i \in (A,I)} E_i(\boldsymbol{r}_A, \boldsymbol{r}_I, \boldsymbol{r}_P) + \sum_{\mu} w_\mu E_\mu, \tag{22}$$

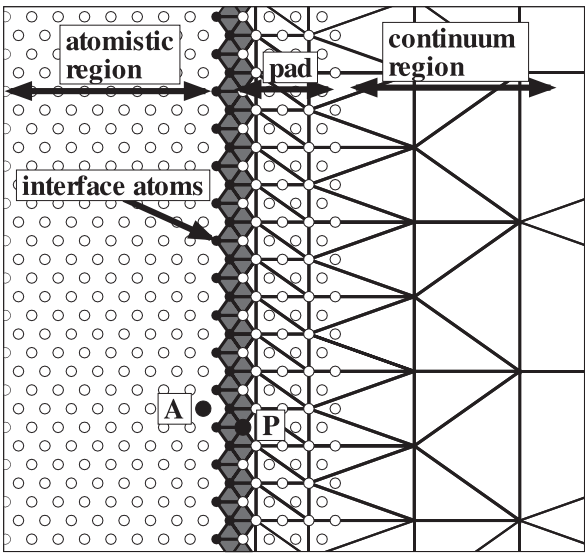

Figure 3. The atomistic/continuum transition region for the QC method. The grey elements do not contribute their full energy to the system because they are tied to interface atoms.

where w_μ is the weight function. w_μ is exactly unity for all elements that are not connected to the interface. For elements connected to the interface, the weight functions depend on the shape of the element, but always satisfy $0 < w_\mu < 1$. For the triangular mesh shown in figure 3, the weight is $w_\mu = \frac{1}{3}$ for elements having two nodes on the interface and $w_\mu = \frac{2}{3}$ for elements having one node on the interface. The energy of each element, E_μ, is obtained via the Cauchy–Born procedure previously described.

The QC implementation can readily be extended to a SW-type atomistic formulation [60, 51, 52]. As noted above, in the case of silicon and other complex-lattice crystal structures, the Cauchy–Born rule is only correct in the limit of small strains, and improvements can be made to consider the effects of the rearrangement of internal degrees of freedom in response to the macroscopically uniform deformation field. With this consideration incorporated into the FE energetics, the total potential energy takes on a form identical to that of equation (22) above, but with the SW atomic energetics for E_i. For the purpose of comparison between the SW QC model and the CLS model of section 3.4, we write the SW QC energy as

$$E_{\mathrm{QC}} = \sum_{i\in(A,I)} E_i^{(2)}(\boldsymbol{r}_A, \boldsymbol{r}_I, \boldsymbol{r}_P) + \sum_{i\in(A,I)} E_i^{(3)}(\boldsymbol{r}_A, \boldsymbol{r}_I, \boldsymbol{r}_P) + \sum_{\mu} w_\mu E_\mu, \tag{23}$$

where the two and three-body contributions are separated.

The QC potential energy leads to some non-physical effects in the transition region, as alluded to in the previous section. Specifically, taking derivatives of the energy functional to obtain forces on atoms and FE nodes leads to so-called ghost forces in the transition region [43, 61]. The origin of these ghost forces lies precisely in the assumption of locality in the continuum region and the local/non-local mismatch in the transition region.

In order to see how the ghost forces arise, it is helpful to consider the situation in which the FE mesh is fully refined in the pad region, so that every node represents a pad atom to avoid the issues associated with interpolation of displacements[4]. Consider the real non-interface atom

[4] The effect of interpolation is only to change the weighting of the relative contributions to the ghost forces. The basic pathology remains unchanged.

labelled A and a pad atom labelled P in figure 3. If the energy functional were fully atomistic, there would be four force terms due to the interactions between these atoms:

1. The force on A from the energy contribution to E_A of pad atom P:

$$\boldsymbol{f}_1 = -\frac{\partial E_A}{\partial \boldsymbol{r}_A}\bigg|_P. \tag{24}$$

2. The force on A from the energy contribution to E_P of atom A:

$$\boldsymbol{f}_2 = -\frac{\partial E_P}{\partial \boldsymbol{r}_A}\bigg|_P. \tag{25}$$

3. The force on P from the energy contribution to P of atom A:

$$\boldsymbol{f}_3 = -\frac{\partial E_P}{\partial \boldsymbol{r}_P}\bigg|_A. \tag{26}$$

4. The force on P from the energy contribtion to A of atom P:

$$\boldsymbol{f}_4 = -\frac{\partial E_A}{\partial \boldsymbol{r}_P}\bigg|_A. \tag{27}$$

If the energy functional were fully continuum, then in equilibrium all of these forces would be zero since the continuum energies are local.

In the QC model, the force $\boldsymbol{f}_2 = 0$ on A, since E_P is not explicitly included in the energy functional—the 'energy of atom P' is contained in a continuum approximation based on the Cauchy–Born rule applied to the deformation at P. Thus, atom A not treated properly as a true atom. Similarly, in the QC formulation the force $\boldsymbol{f}_4 \neq 0$ on P even though P is a continuum node. Thus, P is not treated as a proper continuum node. Overall, in the QC formulation there are forces like $\boldsymbol{f}_2$ that are 'missing' from the atoms near the interface, and forces like $\boldsymbol{f}_4$ on the nodes near the interface that would not arise in a local continuum. These are the so-called 'ghost forces' common to many of the coupled methods discussed herein. Physically, the motion of pad atom P causes a force on atom A but the motion of atom A does not cause a force on P. Enforcing static equilibrium on each atom and FE node leads to a zeroing of the total force on each atom or node. Since these forces are in error, the resulting atom and node displacements are not correct. Errors associated with the ghost forces always exist, independent of the nature of the true deformation. This is most obviously evidenced in the QC model by the existence of small but finite deformations near the transition region in an unstressed perfect crystal [43].

Although the QC method falls into the generic class of problems of interest here, it should be noted that the developers of the QC method are largely responsible for carefully addressing and/or introducing some key general aspects of atomistic/continuum modelling. In particular, the Cauchy–Born approach for calculating $W(\boldsymbol{F}(\boldsymbol{X}))$ in the FE regions via atomistics was introduced by these workers. Furthermore, this unified method of calculating energies based on atomistics alone makes the QC method naturally suited to adaptive re-meshing, i.e. moving the location of the atomistic/continuum boundary and refining or coarsening the continuum domain, during a single simulation. Such adaptive meshing permits the consistent imposition of a maximum allowable error in the energy rather than the typical variation of error associated with a fixed interface. Specifically, the QC method makes use of criteria based on variations in the strain field to expand the atomistically-refined region as necessary, thus tracking the progress of defects and avoiding any bias of the deformation due to the original mesh design. At any stage of adaptation, the QC method still involves an atomistic/continuum interface whose energetics must be defined, and it is this interface that is the focus of our study above.

3.3. The QC method with ghost forces corrected

The spurious interfacial forces in the original QC implementation can be corrected. However, eliminating the ghost forces exactly cannot be done while maintaining a corresponding energy functional for the entire system. Thus, the QC-ghost forces corrected (QC-GFC) is one of the methods where there is no direct coupling in the form of a combined energy functional, and instead the coupling is effected through the simultaneous solution of two separate but overlapping domains. The solution procedure of the FEAt method [40] of section 3.5 and the latest developments of CADD [62] (section 3.7) make use of a coupling procedure similar to that detailed here.

To correct for the ghost forces, one must add or subtract the necessary forces on atoms and nodes in the transition region. The overriding rule is that atoms should 'see', from an energetic point of view, only atoms while continuum nodes should 'see' only continuum nodes. Thus, from the viewpoint of the atomistic domain, the total energy for the atomistic domain and pad atoms should be expressed fully atomistically as

$$E^a = \sum_{i\in(A,I,P)} E_i(\boldsymbol{r}_A, \boldsymbol{r}_I, \boldsymbol{r}_P), \tag{28}$$

where the sum includes the pad atoms, although these are not degrees of freedom. Partial derivatives of E^a with respect to positions $\boldsymbol{r}_A$ then yield full atomistic forces on the atoms. Partial derivatives of E^a with respect to pad atoms P are simply not performed, since the above energy function is relevant only to the 'real' atoms, A. From the viewpoint of the continuum domain, the total energy of the continuum domain (which overlaps the pad atoms) should be expressed as

$$E^c = \sum_{\mu} E_\mu(\boldsymbol{U}_I, \boldsymbol{U}_C), \tag{29}$$

which depends on the nodal displacements of the atom/nodes on the interface, $\boldsymbol{U}_I$ and on the displacements of the rest of the nodes in the continuum, $\boldsymbol{U}_C$. Note that the displacements of the interface atom/nodes are unambiguously determined from the reference crystal and the current atom positions through $\boldsymbol{U}_I = \boldsymbol{r}_I - \boldsymbol{R}_I$. The interface atoms are moved as atoms, i.e. using the forces obtained by differentiating equation (28). In equation (29), the interface nodes are, at each increment, considered fixed nodes with prescribed displacements $\boldsymbol{U}_I$. Thus, the forces on the FE nodes as derived from E^c have no knowledge of the atomic positions $\boldsymbol{r}_A$.

Note that the energy E^a includes the energy of pad atoms whose energy is already implicitly contained in the continuum energy E^c. A true total energy for the system cannot be unambiguously defined. Without a total energy from which forces can be derived, it is not possible to use the computationally-efficient conjugate-gradient method to drive the entire system toward equilibrium. When extended to dynamic approaches, a proper total energy is desirable to monitor stability of the evolving dynamic system and to formally ensure that the model has time-reversal symmetry. Static equilibrium can still be found using the forces only, however, via quasi-Newton methods (which require derivatives of the forces) or by applying the conjugate-gradient method to find a zero of the total force rather than a minimum of the total energy.

Approximate total energy expressions can be constructed by weighting the pad contributions in E^a and E^c and adding the so-modified E^a and E^c together; the QC method uses one such approximate energy expression. However, the forces generated from such an energy functional will retain a fraction of the ghost forces corresponding to the weights used for the pad atoms. Any approach employing a coupled energy functional is therefore a compromise between the accuracy of the results and the need for a well-defined total energy.

An intermediate approach to handling the ghost forces was taken by some developers of the QC model [43]. The exact ghost forces were calculated for the initial reference state of the material system, $\boldsymbol{g}^0$, and then the negatives of these forces were used as constant 'dead loads' applied to the relevant degrees of freedom (atoms and nodes) throughout the entire course of the simulation. With the forces as dead loads, the original QC energy functional is then simply augmented by a term associated with the work done by these dead loads during deformation:

$$E'_{\mathrm{QC}} = E_{\mathrm{QC}} - \sum_g \boldsymbol{g}^0 \cdot \boldsymbol{u}. \tag{30}$$

It is interesting to note that the problem of ghost forces was encountered by Mullins *et al* [11] in their formulation of one of the early coupled methods in the 1980s. The remedy adopted in that early work was essentially the same dead load correction of equation (30).

Because the approximate correction to the ghost forces presented in equation (30) assumes constant $\boldsymbol{g}^0$, a conjugate-gradient method can be applied to minimize the energy. The assumption of constant ghost forces corrects for the major errors occuring at the interface in the usual QC method. However, if the initial deformation across the interface is non-uniform, the ghost force corrections will include some effects not really due to ghost forces alone. Hence, this approach can be useful but can also lead to additional spurious effects. A reasonable strategy for some problems is to calculate the ghost forces for the geometry of interest under stress-free and defect-free conditions. Under subsequent impositions of loads and displacements, residual ghost forces will arise but these will only be roughly proportional to the true displacements. When adaptive meshing is performed such that the local/non-local (or atomistic/FE interface) is changing, such a strategy is not feasible and it is necessary to recalculate the ghost forces after each remeshing step since the atoms/nodes experiencing ghost forces are changing. Such approaches to correcting for the ghost forces thus become computational less tractable and, therefore, less attractive.

3.4. The CLS method

The CLS method of [23, 39, 63, 64] has a transition region that is depicted schematically in figure 4. In CLS, all of the atoms in the pad region are in direct correspondence with nodes of the FE mesh. As in the QC method above, FEs that contact the interface contribute less than their full energy to the total potential energy of the system, and thus these are shaded grey in the figure. In the continuum region, all of the FEs are modelled as linearly elastic, and so the strain energy density in the continuum is given by equation (7). The elastic moduli in $\boldsymbol{C}$ are chosen to exactly match those of the underlying atomistic model, thus minimizing the mismatch across the interface. Using this definition of the strain energy density, the energy of an element is then, from equation (11):

$$E_\mu = \int_{\Omega_\mu} W_{\mathrm{lin}}(\boldsymbol{X})\, \mathrm{d}\boldsymbol{V}. \tag{31}$$

The atomistic energy of the CLS method as applied to Silicon is described by SW-type potentials with two-body and three-body interactions. As well, the CLS method was originally formulated in terms of the energy of each bond in the system, rather than on the atom-by-atom basis adopted here. Specifically, each two-body or three-body bond contributes its full energy to the system if all participants in the bond are in the atomistic region or on the interface ($i \in (I, A)$). If the bond includes one or more atoms from the pad, the contribution is scaled by a factor of $\frac{1}{2}$. Examples of bonds which contribute fully (dark lines) and partially (dashed lines) are shown in figure 4. For the two-body interactions, the above approach is exactly the same as in the QC method in which an atom's site energy is only included if $i \in (I, A)$. This is

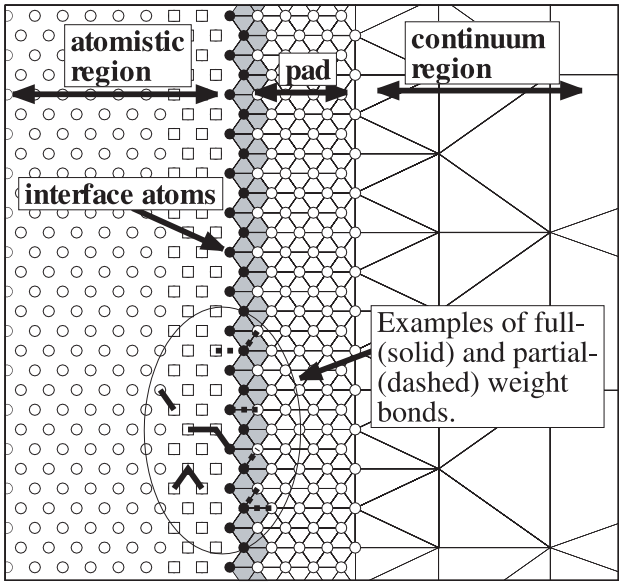

Figure 4. The atomistic/continuum transition region for the CLS method discussed herein. Grey elements contribute $\frac{1}{2}$ of their energy to the system total, as do bonds (dashed) that include both pad atoms and actual atoms. Square atoms have a modified site energy due to their interaction with the pad atoms across the interface.

because in the atom-by-atom energy description, the energy of each two-body bond is divided equally between the two site energies of equation (23). Thus, bonds between two atoms on the atomistic side are fully counted, since both site energies are included, and bonds between true atoms and pad atoms contribute only the half that is part of the true atom site energy. On the other hand, for a QC formulation with a SW atomistic model, three-body bonds which cross the interface would contribute either one-third or two-thirds of their energy depending of whether two or one of the participating atoms were in the pad region.

To write the CLS potential energy in the language of this review, we note that in CLS there is essentially a layer of atoms within $2R_{\text{cut}}$ of the FE region where the three-body contribution to the atom's site energy is modified based on the number of bonds that cross the interface. These atoms are denoted schematically in figure 4 as the squares, and defined here to be the subset A' of the set of all the atoms in the atomistic region A, while the atoms further away from the interface are denoted A'' such that $A' \cup A'' = A$. The potential energy of the CLS model can then be written as

$$E_{\text{CLS}} = \sum_{i\in(A,I)} E_i^{(2)}(\boldsymbol{r}_A, \boldsymbol{r}_I, \boldsymbol{r}_P) + \sum_{i\in(A'')} E_i^{(3)}(\boldsymbol{r}_A, \boldsymbol{r}_I) + \sum_{i\in(A',I)} \hat{E}_i^{(3)}(\boldsymbol{r}_A, \boldsymbol{r}_I, \boldsymbol{r}_P) + \sum_{\mu} w_\mu E_\mu. \tag{32}$$

The weighting factor for the FEs is simply $w_\mu = \frac{1}{2}$ for elements containing an interface atom/node I and unity otherwise. The effect of the partial-weighting of bonds in the three-body interactions is contained in the modified three-body energy, $\hat{E}^{(3)}$, which includes a weight for each bond as follows:

$$\hat{E}_i^{(3)} = \frac{1}{6}\sum_{j\neq i}\sum_{k\neq(i,j)} w_{jk} V_{ijk}^{(3)}(\boldsymbol{r}_{ij}, \boldsymbol{r}_{ik}), \tag{33}$$

where

$$w_{jk} = \begin{cases} 1 & \text{if } (j,k) \in (A,I), \\ \frac{3}{2} & \text{if } (j,k) \notin (A,I), \\ \frac{3}{4} & \text{if } j \in (A,I) \text{ and } k \notin (A,I), \text{ or} \\ \frac{3}{4} & \text{if } k \in (A,I) \text{ and } j \notin (A,I). \end{cases} \tag{34}$$

Written in this way, it is possible to see the similarity between the CLS potential energy of equation (32) and that of the QC method in equation (23). In the limit of small strains in the continuum, such that the linear approximation to E_μ in the CLS coincides with the Cauchy–Born approximation to E_μ in the QC, the only differences are in the weight factors w_μ and w_{jk}. Thus, the same non-physical effects (i.e. ghost forces) of the QC method will be present in the CLS transition zone, but with different magnitudes. In general it is not possible to say whether the QC ghost forces or the CLS ghost forces will be larger, as it will depend on the interatomic potentials and the deformation state, but they are expected to be of the same order of magnitude.

One unique and important feature of the CLS method is that it incorporates the coupling of not only a continuum to an atomistic region described by interatomic potentials, but also the embedding of a TB atomistic region within the classical atomistic region. The details of this 'electronic to atomistic' coupling will not be discussed here. It is sufficient to note, however, that at the interface between a fully quantum description and an interatomic potential description, a transition region exists and the issues in defining such a transition region are nearly identical to those in the fully classical atomistic/continuum interface. One difference is that both quantum mechanics and interatomic potentials are non-local but, since the nature of the non-locality is different, 'ghost forces' and other artefacts can again occur at the interface. An additional subtlety in the quantum problem is that the energy of the system cannot be partitioned on a per-atom basis: the energy is a single quantity that depends on all of the atoms included in the calculation. CLS was also constructed as a dynamic, finite temperature method wherein molecular dynamics methods are used to drive the motion of both atomic and FE degrees of freedom. We will discuss these features later in this review.

3.5. The FEAt model

The FEAt model is historically the earliest of the models discussed in this review, and it is also the only model that attempts to address the problem of a local/non-local mismatch directly through a non-local continuum formulation near the atomistic/continuum interface. The transition region for the FEAt model is shown in figure 5, where the grey elements are elements in the pad region. In the FEAt model, the pad atoms are directly tied to the continuum elements which they overlap. Further, the FE region is resolved down to the atomic-scale in the pad region, which extends to twice the cutoff radius, R_{cut} of the interatomic potentials. In this way, the atoms in the pad directly coincide with nodes in the FE mesh, and atoms in the atomistic region have their full complement of neighbours. Note that the pad must be $2R_{\text{cut}}$ thick because the underlying atomistic model is of the EAM type, and thus atomic forces (derivatives of energy) depend on the electron-density at an atom and at an atom's neighbour R_{cut} away, the latter of which depends on a neighbour's neighbour, up to another R_{cut} away.

Like the QC-GFC model described in section 3.3, the FEAt model does not make use of a unified energy function for the entire coupled problem, but rather effects the coupling through the boundary condition between the atomistic and continuum domains.

The strain energy density in the elements, and therefore the description of E_μ in the FEAt model, is defined in two different ways. Outside of the pad region, non-linear elasticity is

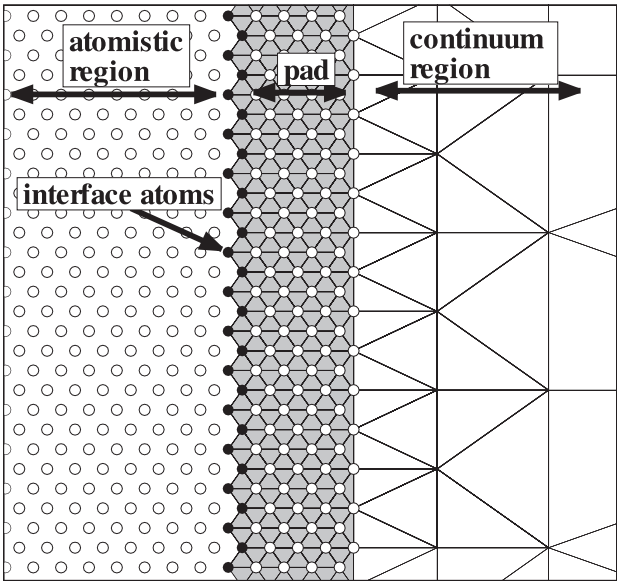

Figure 5. The atomistic/continuum transition region for the FEAt method. Grey elements are treated using non-local elasticity, while the white elements use a more conventional non-linear elastic constitutive law.

used, so that

$$W_{\text{nonlin}}(\boldsymbol{X}) = \tfrac{1}{2}\,[\boldsymbol{C}\cdot\boldsymbol{\epsilon}(\boldsymbol{X})]:\boldsymbol{\epsilon}(\boldsymbol{X}) + \tfrac{1}{6}[\boldsymbol{\epsilon}(\boldsymbol{X})^{\mathrm{T}}\cdot\boldsymbol{C}'\cdot\boldsymbol{\epsilon}(\boldsymbol{X})]:\boldsymbol{\epsilon}(\boldsymbol{X}), \tag{35}$$

where $\boldsymbol{C}'$ (a sixth-order tensor) is the next higher order modulus in the Taylor series expansion of the strain energy. The elastic moduli in $\boldsymbol{C}$ and $\boldsymbol{C}'$ are chosen to exactly match the non-linear response of the underlying atomistic model to second-order, which decreases the mismatch in material constitutive models across the transition region. Using this definition of the strain energy density, the energy of an element from equation (11) is then

$$E_\mu = \int_{\Omega_\mu} W_{\text{nonlin}}(\boldsymbol{X})\,\mathrm{d}\boldsymbol{V}. \tag{36}$$

In an effort to mitigate the effects of the sharp transition from a non-local atomistic region to a local continuum, the FEAt model also uses a non-local continuum formulation to describe the energetics of the elements in the pad region. Thus, for pad elements (the grey elements in figure 5), the strain energy density definition is

$$W_{\text{nonloc}}(\boldsymbol{X}) = \frac{1}{2}\int_{\Omega'} [\boldsymbol{C}^*(\boldsymbol{X}-\boldsymbol{X}')\cdot\boldsymbol{\epsilon}(\boldsymbol{X}')]:\boldsymbol{\epsilon}(\boldsymbol{X})\,\mathrm{d}\boldsymbol{V}', \tag{37}$$

where the integral is over the volume Ω' of whole body (although practical implementations introduce a finite cutoff distance), and $\boldsymbol{C}^*$ is a material-dependent non-local kernel. In these elements the energy is then

$$E_\mu^{(\text{nonloc})} = \int_{\Omega_\mu} W_{\text{nonloc}}(\boldsymbol{X})\,\mathrm{d}\boldsymbol{V}. \tag{38}$$

The energy of the continuum region in the FEAt model is then found by summing the energy the local and non-local FEs

$$E^c_{\text{FEAt}} = \sum_{\mu\in P} E_\mu^{(\text{nonloc})}(\boldsymbol{r}_I, \boldsymbol{r}_P) + \sum_{\mu\notin P} E_\mu^{(\text{nonlin})}, \tag{39}$$

where the dependence of the E_μ on the nodal degrees of freedom is implicit. The energy of the atomistic region is found by the usual sum over atoms, including the pad atoms, as

$$E^a_{\mathrm{FEAt}} = \sum_{i \in A,I,P} E_i(\boldsymbol{r}_A, \boldsymbol{r}_I, \boldsymbol{r}_P), \tag{40}$$

where the positions of the pad atoms provide the neighbour environment for all the atoms in the sum.

Although the FEAt model was formulated based on the EAM atomistic law, introducing the SW law would not introduce any formal difficulties: the EAM energetics would be replaced by the SW energetics and all elastic constants for the continuum would have to be matched to those predicted by the SW model.

Conceptually, the FEAt model is solved iteratively as follows. The interface atoms I are used to provide a boundary condition for the FE model. Solution of the FE model for fixed I atoms provides pad atom positions $\boldsymbol{r}_p$ that are used as fixed boundary atoms for updating the real atoms. A similar algorithm is used in the QC-GFC method, and it should be recognized that an overall minimization of the forces in the problem can be carried out simultaneously without a slow iterative approach to equilibrium.

The FEAt model, in essence, automatically includes the ghost force corrections. The use of a non-local FE should improve the errors associated with gradients in deformation across the interface, but this has not been tested against the local FE, and the details of how the non-local FE performs at the interface were not discussed in the original FEAt work. Calculating the strain gradients near the interface using the atom positions treated as nodes seems feasible but this was simply not made clear.

The FEAt model can be viewed as an intermediary between the QC and CLS models in the way it treats the continuum region. The non-linear elasticity extends the linear elasticity approximation of the CLS toward the fully non-linear and non-convex Cauchy–Born-based energy approximation of the QC model.

3.6. Fully non-local QC

Recently, Knap and Ortiz [41] have proposed a QC formulation that is entirely 'non-local' in that the locality implicit in an FE calculation is eliminated. The overall concept is to use FE ideas to kinematically constrain some atomic positions to node positions but to determine forces from a fully non-local atomistic description at all times and in all regions of space. The Cauchy–Born rule is thus abandoned and forces are calculated from clusters of representative atoms centred on atoms corresponding to FE nodes.

Figure 6 schematically illustrates the QC-FNL approach. To define the degrees of freedom in the problem, a set of nodes is chosen from the underlying perfect lattice. Around each of these nodes, a small cluster of representative atoms is constructed by interpolating the displacements of the FE nodes and deforming the perfect lattice accordingly. Using an appropriate weighting scheme to account for the variable density of nodal points throughout the model, the atom clusters are used to compute nodal forces, which in turn are used to find the equilibrium configuration of the nodal displacements. Physically, the weighting scheme can be interpreted as a way of accounting for the atomic degrees of freedom that have been coarsened out by the FE mesh—the contribution of representative atom i is multiplied by n_i, where n_i is the number of atoms that are being represented by that particular contribution. In regions where atomic-scale detail is required, every atom is chosen to be a node, while in regions that are adequately described by continuum mechanics, the representative clusters are a tiny fraction of the total number of atoms in the region. In the fully refined limit, where every atom is chosen as an FE

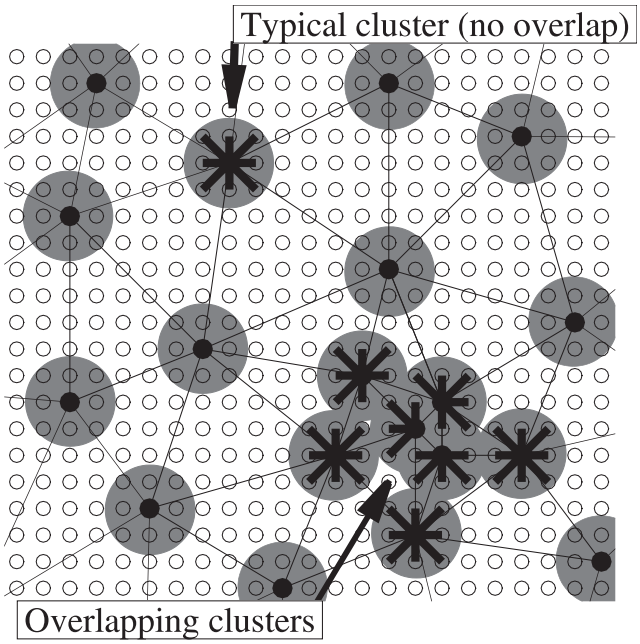

Figure 6. The QC-FNL method. Black atoms are made nodes and represent only the degrees of freedom in the problem. Grey spheres show clusters of representative atoms around each node, used to compute the nodal forces during minimization. Typical clusters in this example, in regions of no overlap, contain 9 atoms as indicated by the heavy lines joining the cluster atoms to the node. In regions where the clusters overlap, cluster size is reduced so that no atom is in more than one cluster. Degeneracies (where a cluster atom is equidistant to two nodes) are resolved randomly.

node, the QC-FNL reduces exactly to the full atomistic simulation dictated by the underlying interatomic potentials. In this limit, there is complete overlap of nearby clusters of atoms, and the counting procedure is designed to account exactly for such overlap.

Here, the QC-FNL approach is outlined briefly, and readers are referred to the original paper [41] for further details. The QC-FNL formulation works directly from an approximate expression for the forces, rather than from the explicit differentiation of an energy functional. Recalling the FE interpolation of equation (13), the positions of all the atoms, $\{\boldsymbol{r}_A\}$, are determined from the reference positions, $\{\boldsymbol{R}_A\}$, and the interpolated displacement field $\boldsymbol{u}$. Thus, derivatives of equation (1) with respect to nodal displacements are

$$\boldsymbol{f}_j \equiv -\frac{\partial E^a}{\partial \boldsymbol{U}_j} = -\sum_{i=1}^{N} \frac{\partial E_i(\boldsymbol{u})}{\partial \boldsymbol{u}} \frac{\partial \boldsymbol{u}}{\partial \boldsymbol{U}_j}, \tag{41}$$

where we recall that the notation $\boldsymbol{u}$ implies the interpolated displacement field and $\boldsymbol{U}_j$ the displacement of a specific node j. Because of equation (13),

$$\frac{\partial \boldsymbol{u}}{\partial \boldsymbol{U}_j} = S_j \boldsymbol{I} \tag{42}$$

and so the force expression becomes

$$\boldsymbol{f}_j = -\sum_{i=1}^{N} \frac{\partial E_i(\boldsymbol{u})}{\partial \boldsymbol{u}} S_j. \tag{43}$$

This summation can be suitably approximated by visiting only a small subset of all the atoms in the problem. Specifically, a cluster of sampling points is defined around each node as shown in figure 6. The forces are then approximated as

$$\boldsymbol{f}_j \approx -\sum_i^N n_i \left[\sum_{c \in \mathcal{C}_i} \boldsymbol{g}_c S_j(\boldsymbol{X}_c) \right], \tag{44}$$

where $\mathcal{C}_j$ refers to the set of atoms in the cluster around node j,

$$\boldsymbol{g}_c = \frac{\partial E^a}{\partial \boldsymbol{u}_c} \tag{45}$$

is the atomic-level force experienced by cluster atom c in displacement field $\boldsymbol{u}$, and n_i is a weight function for node i. The optimal cluster size is a trade-off between computational efficiency and error in the approximation, but was found by Knap and Ortiz [41] to be on the order of first or second neighbour shells.

The QC-FNL method appears promising by virtue of one main advantage: it is truly seamless. This is not strictly true of any of the other methods discussed here, although the respective groups have worked hard to mitigate the effects of the atomistic/continuum transition. In the QC-FNL method, there is simply no transition, and the only error that is introduced is due to the reduction of degrees of freedom in the regions that are sparsely populated with representative atoms. Due to this and the ability of the QC to adaptively refine the mesh during a simulation, the QC-FNL method represents the closest thing to a full coupling of atomistics to continuum. The main disadvantage of the QC-FNL method is the high computational cost in regions of slowly varying deformation gradient as compared to a simple linear elastic constitutive law or even the Cauchy–Born approximation in the local QC.

3.7. The CADD method

All of the above methods restrict the 'interesting' and complex behaviour/deformations to the atomistic region alone. The role of the continuum region is thus primarily to remove the boundaries of the problem far from the deforming atoms and thus permit greatly improved and/or better-defined boundary value problems to be tackled. While powerfully extending the range and accuracy of atomistic methods, these methods are incapable of handling certain inelastic deformations (and specifically plastic flow) at scales larger than a few hundred nanometres. The CADD method of [42] has been designed to permit the existence of continuum dislocations, and thus discrete dislocation plasticity, in the continuum region. The CADD method is thus multi-scale in two ways: at the level of the material description by incorporation of both linear elastic regions and atomistic regions, and at also at the level of defects in that the dislocations are treated differently depending on the region in which they reside. Further, CADD allows for the transfer of dislocations between the atomistic and continuum descriptions as the deformation proceeds. CADD is currently a two-dimensional, static formalism due to the difficulties in transferring dislocations across the atomistic/continuum boundary in three-dimensional. A related approach was developed by Yang *et al* [65] for treating fracture and another method was developed by [66] that contains useful insights but lacks the practical applicability of the more recent method.

The idea of the CADD method is illustrated in figure 7, where the typical problem of a continuum region coupled to an atomistic region is shown in the top left. The difference is that the continuum region can contain continuum dislocations that move in response to stress, as illustrated schematically. The coupled problem is solved by cutting the problem into two parts at the atomistic/continuum interface and enforcing compatibility by tying the interface

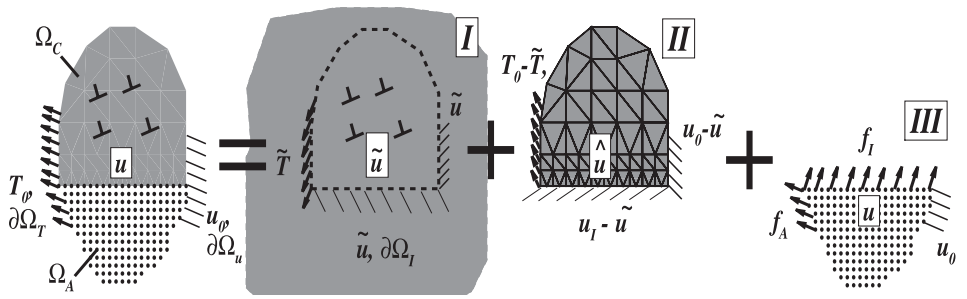

Figure 7. Schematic of the CADD method for coupling an atomistic region to a continuum region containing discrete dislocations. Note that for clarity, the 'pad' atoms discussed in the text are not shown.

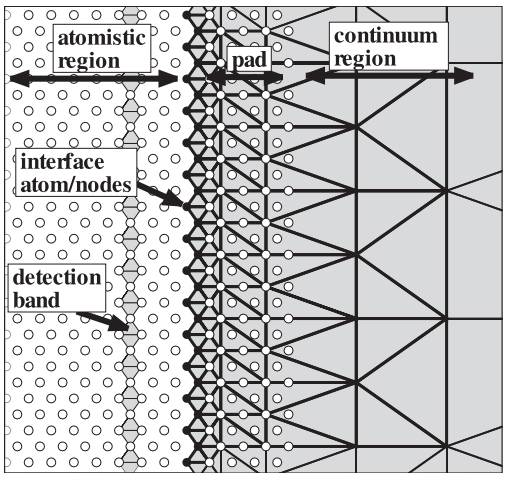

Figure 8. Schematic of the transition region used in the CADD method. The detection band in the atomistic region (dark grey) is used to detect slip.

nodes in the continuum to the interface atoms. The continuum problem with any number of discrete dislocations can then be efficiently solved using the method of [3], whereby the solution is found as the superposition (problems I and II of figure 7) of the dislocation fields in an infinite continuum, denoted as $\tilde{\boldsymbol{\sigma}}$ and $\tilde{\boldsymbol{\epsilon}}$, and an appropriate corrective field, denoted as $\hat{\boldsymbol{\sigma}}$ and $\hat{\boldsymbol{\epsilon}}$, that is obtained by solving a boundary value problem with boundary conditions chosen so that the superposition of the ˆ-fields and ˜-fields matches the true boundary conditions in the problem. The dislocation fields are known analytically and contain all the singularities and discontinuities in the problem so that the remaining corrective solution is smooth, continuous and ideally suited to FE.

The CADD approach has an atomistic/continuum transition region that can be handled in any convenient manner, including those discussed in the QC, QC-GFC and CLS methods above. In [42], an alternative method was developed that retained an energy functional for the problem, as follows. The transition is as depicted in figure 8(*a*). Rather than tying the pad atoms to the continuum deformation (i.e. determining the $\boldsymbol{r}_P$ from the FE nodal displacements), the pad atoms are not connected to the continuum deformation. The role of the pad atoms in CADD is simply to mitigate the effect of the free surface that would be created on the atomistic

region during the cutting process shown in figure 7. This introduces an error by counting the atomistic energy of (modestly deformed) material in the pad region, and makes the transition region artificially stiff against stretching along the interface. However, this approach moves the free surface away from the interface, allowing atoms in the atomistic region and on the interface to behave more like true 'bulk' atoms. In this formulation, the FE problem is solved with fixed interface displacements U_I at each increment, leading to tractions T_I that are applied as forces f_I on the interface atoms. The interface atoms are then moved by the forces from the real atoms, the pad atoms and the f_I. The energy functional thus takes the form

$$E_{\mathrm{CADD}} = \sum_{i\in(A,I,P)} E_i(\boldsymbol{r}_A, \boldsymbol{r}_I, \boldsymbol{r}_P) + E^c, \tag{46}$$

where the continuum energy E_c in the presence of the continuum dislocations is described more fully below. This published implementation of the CADD interface coupling suffers from some of the same 'ghost-force-like' problems of the QC and CLS methods, as will be seen in the next section. Recent work by the authors [62] has proceeded to implement the equivalent of the QC-GFC transition region within the CADD method, however.

The presence of the dislocations in the continuum leads to a slightly more complex energy functional E^c, taking the form

$$E^c = \frac{1}{2}\int_{\Omega_C} (\tilde{\boldsymbol{\sigma}} + \hat{\boldsymbol{\sigma}}) : (\tilde{\boldsymbol{\epsilon}} + \hat{\boldsymbol{\epsilon}})\, \mathrm{d}\boldsymbol{V} \tag{47}$$

in the absense of any externally applied loads. This integral contains three types of terms, those involving only the analytic $\tilde{}$ fields, those involving only the corrective $\hat{}$ fields, and the cross-terms. The integration of the $\tilde{}$ field terms requires special care because of the discontinuities in the dislocation fields, but can be accurately and efficiently computed by making use of the Airy stress function χ for the stress field $\tilde{\boldsymbol{\sigma}}$. The integral over the volume is then replaced by an integral over the boundary of the continuum region as

$$\int_{\Omega_C} (\tilde{\boldsymbol{\sigma}} : \tilde{\boldsymbol{\epsilon}})\, \mathrm{d}\boldsymbol{V} = \sum_{i=1}^{ND} \left(\frac{\partial \chi_i'(d^i)}{\partial y} b_x^i - \frac{\partial \chi_i'(\boldsymbol{d}^i)}{\partial x} b_y^i \right) - 2\int_{\partial\Omega} \left[\left(\frac{\partial \chi}{\partial y} \right) \boldsymbol{\nabla} \tilde{u}_x - \left(\frac{\partial \chi}{\partial x} \right) \boldsymbol{\nabla} \tilde{u}_y \right] \mathrm{d}\gamma, \tag{48}$$

where $\chi_i'(\boldsymbol{d}^i)$ is the stress function for all but the ith dislocation evaluated at the location $\boldsymbol{d}^i$, of dislocation i, $\boldsymbol{b}$ is the Burgers vector, $\boldsymbol{u}$ is the displacement field along the boundary, and ND is the number of dislocations. The cross-terms between the $\tilde{}$ and $\hat{}$ fields can be treated using Green's theorem to replace the volume integrals with integrals of the traction times displacements over the boundary of the continuum region, while the terms involving only the $\hat{}$ fields, because they are smooth fields, can be treated in a conventional way. Thus, the continuum energy becomes

$$E^c = \frac{1}{2}\int_{\Omega_C} (\tilde{\boldsymbol{\sigma}} : \tilde{\boldsymbol{\epsilon}})\, \mathrm{d}\boldsymbol{V} + \tilde{\boldsymbol{t}}_I \cdot \hat{\boldsymbol{u}}_I + \sum_{\mu}^{N_{\mathrm{elements}}} E_\mu, \tag{49}$$

where the integral is evaluated using equation (48), the $\boldsymbol{t}\cdot\boldsymbol{u}$ terms are the discretized statement of the surface integrals of traction times displacement, and E_μ is the usual linear elastic energy due to the $\hat{}$ fields:

$$E_\mu = \frac{1}{2}\int_{\Omega_\mu} [(\boldsymbol{C}\cdot\hat{\boldsymbol{\epsilon}}) : \hat{\boldsymbol{\epsilon}}]\, \mathrm{d}\boldsymbol{V}. \tag{50}$$

Combining these continuum contributions with the atomistic energy, the total potential energy of the CADD model of [42] is then

$$E_{\mathrm{CADD}} = \sum_{i\in(A,I,P)} E_i(\boldsymbol{r}_A, \boldsymbol{r}_I, \boldsymbol{r}_P) + \frac{1}{2}\int_{\Omega_C} (\tilde{\boldsymbol{\sigma}} : \tilde{\boldsymbol{\epsilon}})\, \mathrm{d}\boldsymbol{V} + \tilde{\boldsymbol{t}}_I \cdot \hat{\boldsymbol{u}}_I + \sum_{\mu=1}^{N_{\mathrm{elements}}} E_\mu. \tag{51}$$

A major focus in the CADD development was on an important issue missing from all prior methods: the ability to detect and pass dislocations as they move between the atomistic and continuum. Here, we provide a brief discussion of the detection and passing, and refer interested readers to the original publications. Dislocations nucleated in the atomistics and approaching the continuum region must be detected and 'passed' to the continuum region as discrete dislocations. Detection is accomplished by defining a detection band of triangular elements inside the atomistic region, as shown in figure 8 and monitoring the continuum Lagrangian finite strain $\boldsymbol{E}$ in these elements. $\boldsymbol{E}$ is given by

$$\boldsymbol{E} = \frac{(\boldsymbol{b}\otimes\boldsymbol{m})_{\mathrm{sym}}}{d} + \frac{(\boldsymbol{m}\otimes\boldsymbol{b})(\boldsymbol{b}\otimes\boldsymbol{m})}{2d^2}, \tag{52}$$

where $_{\mathrm{sym}}$ implies the symmetric part of a matrix, $\boldsymbol{m}$ is the slip plane normal, $\boldsymbol{b}$ is the Burgers vector and d is the interplanar spacing. Since all the possible slip systems and associated strains $\boldsymbol{E}_i$ are known for a given crystal structure and orientation, when the strain $\boldsymbol{E}$ in any detection band element becomes closer to any $\boldsymbol{E}_i$ than to zero, a dislocation core, with known slip plane and Burgers vector, is assumed to reside at the centroid of that element. A dislocation so identified is passed to the continuum as a discrete dislocation by adding the displacement field of a dislocation dipole with one dislocation at the detection band and the other at a position along the slip plane but in the continuum region. These displacements cancel the original core in the atomistic region and add a new core in the continuum region, which is treated as a discrete dislocation. A short relaxation algorithm anneals out the remnants of the atomic core and moves the continuum dislocation to its equilibrium position. Detecting and passing dislocations from the continuum region back to the atomistics is more easily accomplished.

3.8. An illustrative one-dimensional model

Although some of the methods above do eliminate ghost forces and some other artefacts, it is important to recall that the standard continuum models contain an underlying assumption of uniform deformation that introduces errors associated with the gradient of the deformation gradient. It is therefore useful to demonstrate the effects of the local/non-local mismatch and the other artefacts in some of these models via a simple one-dimensional chain of atoms. Although there are certain limitations to a one-dimensional model, the effects demonstrated here also occur in the simple uniaxial deformation of a three-dimensional material with a planar atomistic/continuum interface perpendicular to the axis of the uniaxial loading, as in figures 2–5.

The underlying interatomic interactions in the one-dimensional chain of atoms are taken to be linear springs connecting first and second neighbours along the chain. The presence of second-neighbour interactions constitutes the non-locality of the atomic problem. The spring constant for first-neighbour interactions is denoted k_1 and that for second-neighbour interactions k_2. A zero-force spring length of a is assumed for the near neighbour springs and of $2a$ for the second neighbour springs. Thus, the unstressed reference crystal corresponds to a chain of atoms with lattice constant a. The energy functional for the chain of atoms can be written in terms of the displacements u_i of the atoms from their original lattice sites as

$$E^a = \sum_i E_i^a, \tag{53}$$

where

$$E_i^a = \tfrac{1}{2}[\tfrac{1}{2}k_1(u_i - u_{i-1})^2 + \tfrac{1}{2}k_1(u_{i+1} - u_i)^2 + \tfrac{1}{2}k_2(u_i - u_{i-2})^2 + \tfrac{1}{2}k_2(u_{i+2} - u_i)^2] \tag{54}$$

with the overall factor of $\frac{1}{2}$ accounting for the double counting of spring energies in the sum over i in equation (54).

An appropriate continuum model of the one-dimensional chain is constructed by considering an elastic energy density functional of the form

$$W = \tfrac{1}{2}C_c\epsilon^2, \tag{55}$$

where C_c is the appropriate elastic constant and ϵ is the strain. In the one-dimensional chain with each atom corresponding to a continuum node, the strain within the element bounded by nodes i and $i-1$ is $\epsilon = (u_i - u_{i-1})/a$. The energy of element i, the integral of i over the element length, is thus

$$E_i^c = \tfrac{1}{2}k_c(u_i - u_{i-1})^2, \tag{56}$$

where $k_c = C_c a$ is the effective spring constant of the element and the convention is to number nodes incrementally from left to right. The total continuum energy is then

$$E^c = \sum_i E_i^c. \tag{57}$$

To determine the proper value for k_c, a state of uniform deformation ($u_i - u_{i-1} = U$) is considered and the energy of the continuum system is matched to that of the fully atomistic system. Setting E_i^c equal to E_i^a for the case of uniform deformation yields

$$k_c = k_1 + 4k_2. \tag{58}$$

With this choice for k_c, the continuum model perfectly predicts the state of deformation of the system under any uniform applied load.

With the atomistic and continuum systems defined above, we now consider the coupled atomistic/continuum models described above within the context of the one-dimensional model. The coupled model corresponds to a chain of atoms/nodes with either first and second neighbour spring interactions (atoms) or only first-neighbour spring interactions (nodes). At the interface where the description changes from atoms to nodes, some admixture of these various springs is considered, as follows.

For the QC model, the energy is a sum over the energies of the atoms and nodes. Denoting the interface atom as I, the energy for the system is then

$$E_{\mathrm{QC}} = \sum_{i \leqslant I} E_i^a + \frac{1}{2}E_{I+1}^c + \sum_{i > I+1} E_i^c, \tag{59}$$

where the weight function of $w_\mu = \frac{1}{2}$ is used for the element adjacent to the interface. The CLS model is identical to the QC model for this simple problem.

For the QC-GFC method, there are two coupled problems to solve with the two energy functionals

$$E^a = \sum_{i \leqslant I+2} E_i^a, \tag{60}$$

$$E^c = \sum_{i > I} E_i^c, \tag{61}$$

where the atomistic sum extends out to $I + 2$ due to the second-neighbour range of the interatomic interactions. Note that the minimization of energy E^a in equation (60) is only

over $i \leqslant I$ with the positions of atoms $I+1$ and $I+2$ fixed by the continuum nodal solutions. Similarly, E^c is constrained such that the position of node I is fixed by the atomistic solution. For the FEAt method without the non-local and non-linear continuum approximations, the energy is identical to the QC-GFC model.

In the QC-FNL model of Knap and Ortiz [41] discussed in section 3.6, there is no clear 'transition region' as in the other methods. The approximations in the QC-FNL come from the discretization of the problem and the varying sizes of the FEs. For this reason, the QC-FNL model is exact for the one-dimensional chain problem with next-near-neighbour interactions.

The transition region adopted in the CADD model contains the pad atoms $I+1$ and $I+2$ that are not connected to the corresponding continuum nodes $I+1$ and $I+2$ and are thus extra degrees of freedom in the problem. Thus, the energy for the entire problem is written as

$$E_{\mathrm{CADD}} = \sum_{i \leqslant I+2} E_i^a + \sum_{i>I} E_i^c, \tag{62}$$

which is minimized with respect to the real atoms, the two pad atoms, and all the continuum nodes. The displacements of the two pad atoms are physically irrelevant, however; they simply 'saturate' the bonds of the real atoms at the interface.

For a chain of 101 atoms at initial positions $r_i = ia$, $i = 0$–100 and with the interface at $I = 50$, we have examined the deformations associated with various applied loadings. In all cases, the displacement of atom 0 is fixed and a force $f = 1$ is applied to atom 100. Figure 9(a) shows the local strain $(u_i - u_{i-1})/a$ between neighbouring atoms or nodes near the transition region of the full atomistic model, the QC/CLS, the QC-GFC/FEAt and CADD models. The QC/CLS model shows unphysical deformations of the atoms/nodes in the transition region due to the existence of the ghost forces. The QC-GFC/FEAt model gives perfect agreement with the atomistics under uniform deformation. The CADD model shows results qualitatively similar, but quantitatively different from, the QC/CLS model.

We now consider inhomogeneous deformations. In a one-dimensional model, inhomogeneous deformation is obtained by explicitly applying point forces on specific atoms or nodes. Here, we create a gradient in the deformation by applying additional forces of magnitude $f = 0.1$ to atoms/nodes $I-2$, $I-1$, I, $I+1$, $I+2$ (with $I = 50$) across the transition region while maintaining the overall applied force of $f = 1$ on atom/node 100. In the CADD model, the pad atoms $I+1$ and $I+2$ have no applied forces. Note that since this system is linear, the applied force $f = 1$ yields deformations that superimpose upon the deformations caused by the smaller distributed point forces. The deformations in each case are shown in figure 9; in the presence of the inhomogeneous deformation, none of the methods reproduce the full atomistics exactly although the QC-GFC/FEAt model agrees well. Due to linearity, the magnitude of the errors scales with the magnitude of the applied forces. The QC/CLS errors are different from those in figure 9(a), showing the general difficulty the prevailing atomistic/continuum coupling methods in accomodating gradients in deformation across the interface.

The QC-GFC/FEAt method results in the presence of inhomogeneous deformation appear reasonable. However, this is due to the cancellation of rather large errors caused by each of the individual point forces. For a single point force applied to an atom or node at the interface, the QC-GFC/FEAt method leads to long-ranged forces and deformations in the atomistic material, as shown in figure 9(c). These errors arise because in the QC-GFC/FEAt approach, there is no strict requirement of self-equilibration of the local forces; the discontinuity in treatment of the atoms and nodes leads to unbalanced forces that are then balanced by long-range forces. When the deformation is not atomistically abrupt, the errors induced on either side of the

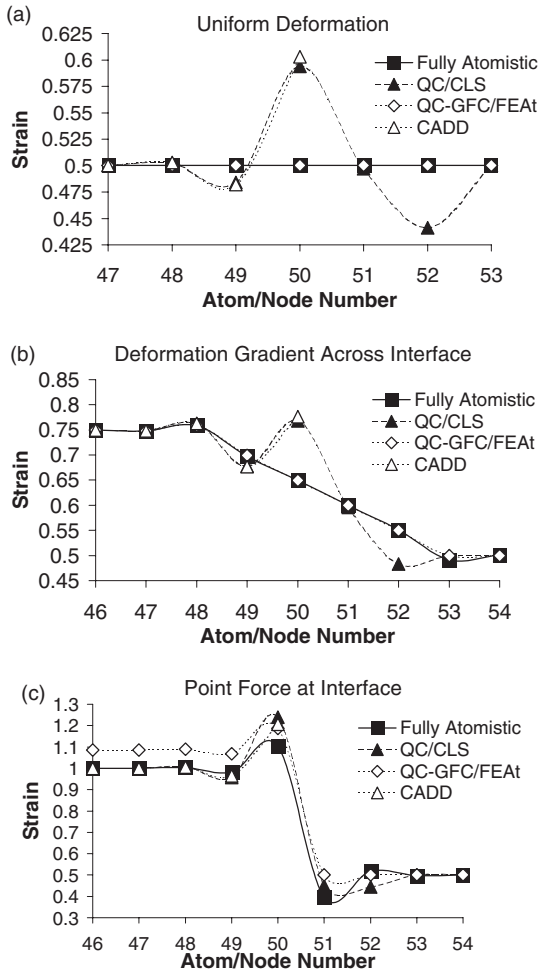

Figure 9. Results of simple one-dimensional model to compare the transition regions of the various models. The CADD model is identical to the QC-GFC/FEAt model in the continuum region and is thus not shown in this region. (*a*) Uniform deformations of the purely atomistic model are reproduced only by the QC-GFC model. (*b*) Errors in the models in the presence of non-uniform deformation. (*c*) Errors in the model in the presence of a single point force applied at the interface.

transition region appear to strongly cancel, leading to good overall results. The QC/CLS and CADD models, in contrast, have displacement errors under homogeneous deformation but do not create any long-range errors even under conditions of atomistically sharp gradients in deformation across the interface.

The one-dimensional model thus demonstrates the two classes of models, and shows that both classes of models have benefits and faults. The QC-GFC/FEAt model appears superior under uniform deformations but the existence of extended corrective forces under sharp gradients in deformation might lead to subtle changes in predicted behaviour. The full non-local FEAt model might decrease this latter problem to some degree but likely will not eliminate it exactly. The QC/CLS and CADD models show a permanent distortion near the interface but do not cause errors in the long-range fields in the presence of gradients. The

preferrable choice of method thus depends on the nature of the problem under investigation and the feasibility of keeping the transition region far from any relevant or important deformations occuring in the atomistic region.

4. Dynamic coupling and finite temperatures

The previous discussion has focussed on molecular statics or zero-temperature equilibrium. There has been a parallel drive toward the development of coupled atomistic/continuum molecular dynamics methods, and work to extend the zero-temperature results to finite temperatures at thermodynamic equilibrium. Here, we very briefly note some of the recent efforts that have emerged to deal with these issues.

The general problem with coupled dynamic models is the treatment of the dynamics of the continuum region and the mismatch in wave spectra between fine and coarse scale descriptions of material. In general, molecular dynamics can be performed using the schemes above simply by solving $\boldsymbol{F} = m\boldsymbol{a}$ for the atoms and using a lumped-mass approximation for the dynamics of the continuum FEs. Such an approach neglects the important physics of dynamic energy transfer across the interface. The discrete atomic system has a wave spectrum with non-linear dispersion that extends up to high frequencies. The (elastic) continuum region is a linear medium and the frequencies supportable by an element are limited by the element size. Hence, heat transfer across the atomistic/continuum boundary is not seamless. There is an interface thermal impedance. Some waves impinging from the atomistic region are unphysically reflected back into the atomistics.

The CLS model is the only model, of those discussed herein, in which molecular dynamics has been implemented. Because the CLS method is a finite temperature, dynamic method, there are additional considerations required to treat the transfer of thermal energy across the interface. Specifically, forces are added to the FE nodes that can be divided into random forces and dissipative forces. These are meant to approximate dissipative effects due to anharmonic interactions with the short-wavelength degrees of freedom that have been removed from the model in order to facilitate the continuum formulation.

Rudd and Broughton [67] recognize that the continuum-based origins of the FE method lead to difficulties in a smooth transition from the atomistic to the continuum when temperature effects are important. Thus, they have reformulated the continuum region using a method called coarse-grain molecular dynamics (CGMD), in which the degrees of freedom reduction is developed as a more natural extension of the underlying discrete molecular dynamics. The CGMD provides a replacement for the FE mesh typically used outside the atomistic region in coupled methods. Currently, the CGMD results have been limited to validation problems that demonstrate the principles of the method, but these initial results are encouraging and addition applications are an area of active research.

Other work has been aimed at developing effective boundary conditions at the atomistic/continuum interface to eliminate the artificial reflections. Cai *et al* [68] developed Green's function method to dynamically couple the two regions. Subsequently E *et al* [69] developed a related but perhaps more practical approach in which the degree of reflection is minimized across the wave spectrum by introducing modified equations of motion for the atoms near the interface. These methods hold promise but have not been fully explored nor extended beyond relatively simple test problems.

Full molecular dynamics includes the thermodynamics of finite temperature, but it can also be fruitful to consider the simpler problem of thermodynamic equilibrium at finite temperature. The goal in such an effort is to accurately capture the free energy of the system at finite T and thus predict thermal properties and behaviour at finite temperatures in which

dissipation and thermally activated phenomena are not relevant, such as thermal expansion and thermoelasticity. To this end, a finite-temperature QC model was developed by [58] in which a local quasiharmonic model for the atomistic free energy developed earlier by Lesar *et al* [70] is employed to calculate free energies. Since the QC uses the Cauchy–Born method to obtain the continuum energies, the temperature dependence of the continuum region is found in a natural manner that is completely consistent with the atomistic model. The quasiharmonic approximation loses accuracy with increasing temperature, however, and so is applicable only at moderate temperatures, relative to the melting point. Operationally, the local harmonic model requires the calculation of the instantaneous vibration frequency of each atom in the environment of fixed surrounding atoms during free energy minimization. Two related problems can thus arise with this model. First, during free energy minimization, some atoms may have negative frequencies (i.e. they are in unstable positions) so that the free energy cannot be calculated, a conjugate-gradient method cannot be applied, and the system cannot be properly driven to equilibrium. Second, it is possible that some true thermodyanamic equilibrium states might be unstable within the local quasiharmonic approximation, and hence unobtainable within such a model.

A renormalization method for heterogeneously coarse-graining an atomistic system while retaining the full thermodynamics has been developed by Curtaloro and Ceder [71] for a simple system of atoms connected by springs in a two-dimensional lattice. In this approach, as in QC, some regions of the material remain fully atomistic while other regions have been coarsened by systematic elimination of degrees of freedom. During the renormalization or coarse graining, the free energy contributions of the internal degrees of freedom are retained on average through an additional term entering the renormalized Hamiltonian. This preserves the average fluctations of the internal degrees of freedom and thus retains the entropy that is often discarded in coarse-graining steps. The prediction of thermodynamic equilibrium quantities in this method coincides well with the full atomistics. It is unclear how to extend this method to more-realistic interatomic interactions such as those obtained from EAM, although once the coarse-graining extends beyond the scale R_{cut} of the real interatomic interactions, the renormalized Hamiltonian should be similar to that for non-linear springs. In extending the method to dynamics, and Curtaloro and Ceder [71] have introduced the dynamical exponent associated with the renormalization of time and obtained this exponent via a fitting procedure. The dynamical coarse-graining does not solve the generic issue noted above regarding heat transport, however; a thermal impedance arises that can be minimized, but not eliminated, at considerable computational cost.

5. Some applications

This review has focused on the atomistic/continuum coupling methods that have been developed. Here, we note some of the problems to which these various methods have been applied. Our aim is to show a variety of problems rather than to review the physics and insight that has emerged from each of these studies, which is far better presented in the original papers.

Fracture has been a phenomenon of interest for many of the coupled methods, due to its inherently multi-scale nature and the need for both realistic boundary conditions and accurate physics at the crack tip. The careful treatment in FEAt of the continuum and interface was employed to calculate the critical energy release rates for fracture and crack tip blunting, allowing for a systematic comparison between the atomistic simulations and continuum-based criteria predicting brittle versus ductile response [72].

Fracture was again the initial application of the CLS method [23, 39, 63], which has since taken advantage of powerful parallel computing to model fully three-dimensional problems

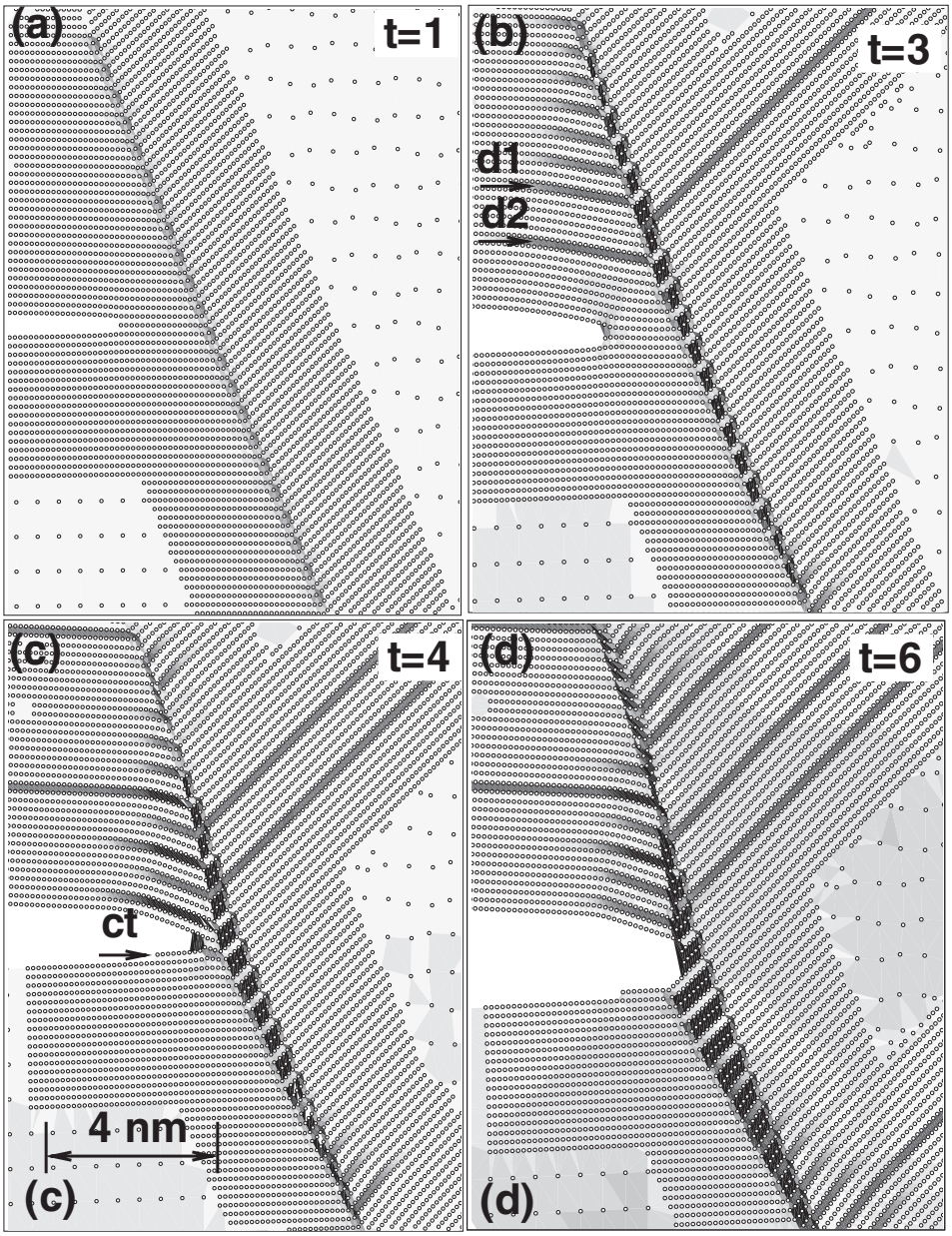

Figure 10. A QC simulation of a crack impinging on a grain boundary. (*a*)–(*d*) Equilibrium atomistic configurations with increasing load levels. Note the adaptive expansion of the atomistic region as defects are emitted from the boundary. Reprinted from [44].

of MEMS resonators [73, 64]. An example of the three-dimensional resonator simulation is shown in figures 1 and 4 of [73], which was used to study the dynamic response of the structure and its nano-scale contributions to dissipation. This development is significant, in that it represents a simulation of an entire (albeit small) engineered device, in contrast to the simulation of basic deformation phenomena typically investigated.

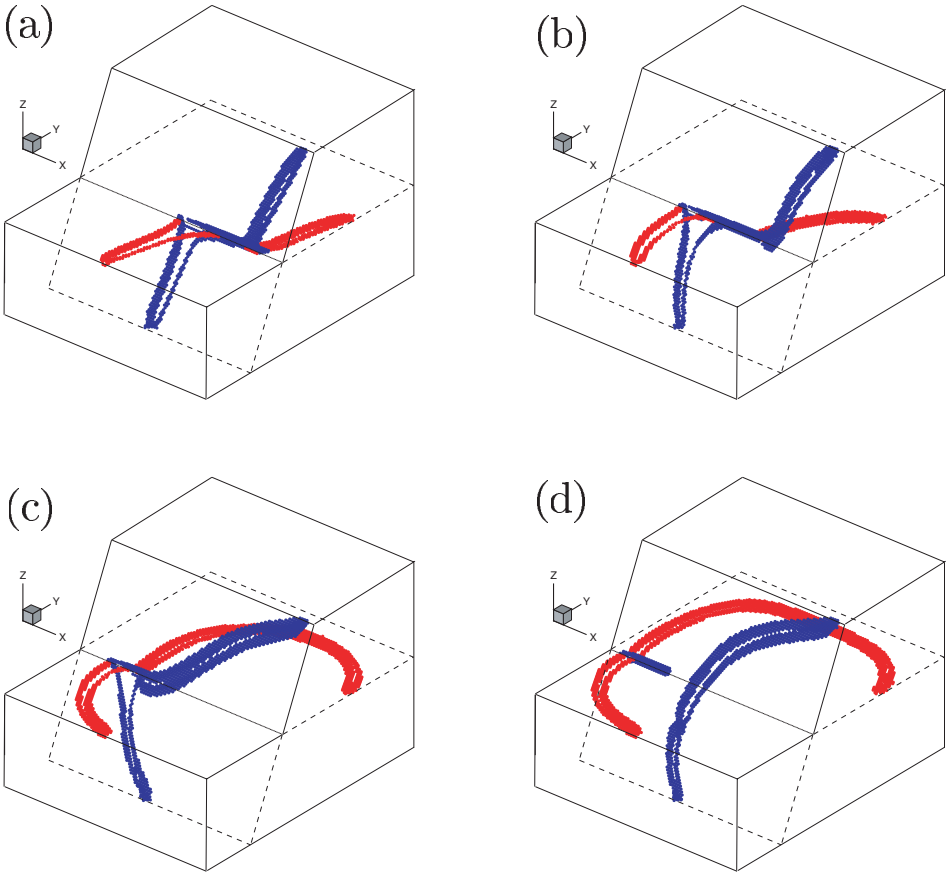

Figure 11. A three-dimensional QC simulation of a dislocation junction. (*a*)–(*d*) Equilibrium configurations with increasing level of applied shear stress. The unstressed junction in (*a*) stretches and moves as the load is increased through (*b*) and (*c*), until the junction finally breaks in (*d*). Reprinted from [54].

The QC method of [37, 43, 38] has been used to investigate a wide range of problems including fracture [44, 45], nano-indentation [48, 50, 49, 41], three-dimensional dislocation junctions [54] and grain boundary structure [38, 61]. The method is well-suited to automatic mesh adaption, allowing it to expand the atomistic region as required to track the progress of defects. Figure 10 shows a QC simulation of a crack impinging on a grain boundary, each frame presenting a close-up of the atomistic region which is embedded in a much larger continuum. The figures are of relaxed equilibrium configurations for particular load-steps, denoted by the relative timescale in the upper right. This particular grain boundary and crystal orientation lead to the emission of dislocations from the boundary, and a migration of the boundary itself due to the high stresses near the crack tip. Finally, the crack tip is blunted when it advances to the boundary plane. Figure 11 shows a fully three-dimensional implementation of the QC method used to study the strength of dislocation junctions in fcc Al.

The CADD method was first applied to a simple two-dimensional nano-indentation problem and compared against full atomistics on a problem sized to be accessible using atomistics. Figure 12 shows the sample geometry, the rigid indenter and the fully atomistic region as a small box located near the indenter corner, where dislocation nucleation will

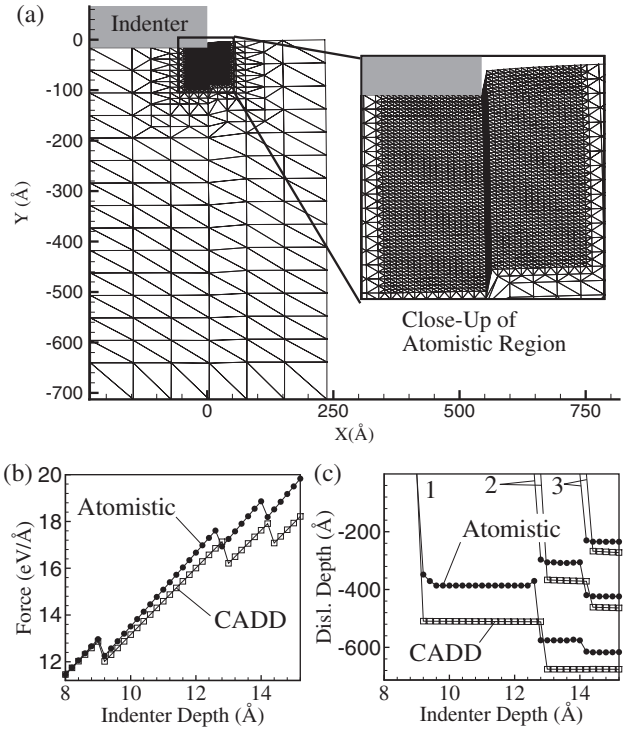

Figure 12. (*a*) CADD mesh used to simulate nano-indentation. A deformed FE mesh is used in the atomistic regime and shows where slip has occurred. (*b*) Applied load and (*c*) positions of first three emitted dislocations (labelled 1, 2 and 3) as a function of indenter displacement. □: CADD results; ●: full atomistics.

occur. The CADD problem contains only about 3000 atoms/nodes (2800 atoms and 200 FE nodes) whereas the full atomistic problem contains about 100 000 atoms. Under indentation, dislocations are nucleated, move away from the indenter into the continuum, and exert a back stress on the atoms near the indenter corner. The predicted force-displacement behaviour and the positions of nucleated dislocations are shown in figures 12(*b*) and (*c*), and compare favourably to the atomistic results also presented. The differences in dislocation position are largely associated with the very shallow energy minima for the dislocations in the continuum region, which leads to relatively large differences in position caused by small errors in the predicted stress fields.

The CADD method, with a transition region following the QC-GFC method rather than the prior free-floating pad approach, has recently been applied to the problem of two-dimensional Brinell indentation, i.e. indentation by a frictionless cylindrical indenter in correspondence with the usual three-dimensional Brinell test using a spherical indenter. Figure 13 shows one result of such a simulation. In (*a*), the load-displacement curve is shown and indicates the points of the first dislocation nucleation (*I*), maximum load (*II*) and complete unloading (*III*). Dislocations are nucleated below the indenter in the atomistic region, and travel to the locations shown in (*b*) where they pile up against the constrained lower surface of the region. Other dislocations move toward the upper free surface, are deflected by the indenter, and move laterally. The non-linear deformation thus occurs within large volumes that could

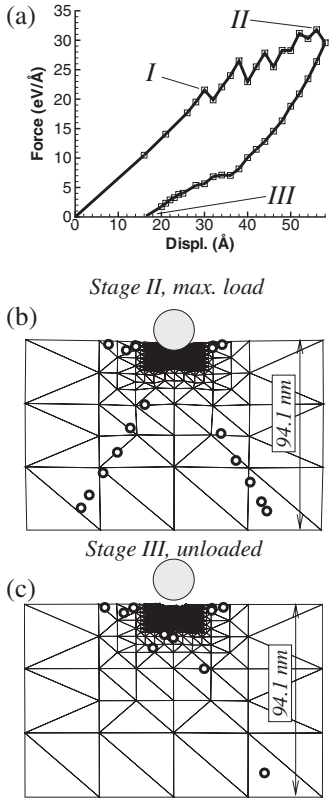

Figure 13. A CADD simulation of indentation by a spherical indenter. The load-displacement curve is shown in (*a*), while the deformed mesh and locations of the discrete dislocations (○) are shown at maximum load in (*b*) and after unloading in (*c*).

not be handled by full atomistics. Upon unloading in (*c*), some of the dislocations in the continuum move back into the atomistic domain. Some annihilation occurs and some permanent deformation (the indent) remains on full unloading. The ability of CADD to capture complex deformation, nucleation, annihilation and flow of dislocations back and forth across the atomistic/continuum boundary is encouraging for future applications to a wide range of other problems. CADD is generally well-suited to problems where nucleation requires full atomic resolution but deformation (dislocation motion) occurs over large volumes that is adequately captured by treating the dislocations as continuum entities.

6. Concluding remarks

This review has compared several different atomistic-continuum coupling methods using a common language and notation. The comparison sheds light on the main differences and similarities between the methods, and introduces newcomers to the essential features and limitations of such approaches.

Recall that an ideal goal is to simulate the behaviour of materials with the only constitutive law being the interactions between the atoms. But due to the scales of deformation that are important in realistic problems, explicit modelling of all of the atomic degrees of freedom will

never be feasible. Thus, one must selectively remove most of these degrees of freedom to make the problem tractable. The vehicle for this reduction of degrees of freedom is the continuum, where for crystalline materials the atomic positions can be tracked via displacement fields interpolated between a sparse set of nodes. The difficulty then lies in the intimate and accurate coupling of continuum and atomistic regions so that the atomistic region behaves as if the entire model is atomistic. The methods reviewed here achieve this goal to varying degrees, through a blend of art and science aiming to achieve accurate, if not exact, coupling within a tractable and implementable framework. The current methods represent computational tools that can be used to provide some answers to questions of materials science that until recently remained elusive. These methods are also providing a basis for pushing forward with new models that expand modelling capabilites further to include important phenomena such as heat transport, dislocation plasticity, and quantum mechanics. These multi-scale models will not replace the hierarchical approach of passing information from one scale to the next. Rather, the intrinsically multi-scale models will complement the hierarchical models by eliminating information passing in some cases and by permitting accurate assessment of the validity of information passing in a broad spectrum of problems. In tandem, these approaches hold great promise for the continued advancement of computational materials science.

Acknowledgments

The authors ackowledge support from the US AFOSR through the MURI Program 'Virtual Design and Testing of Materials: a Multi-Scale Approach' at Brown University. WAC also acknowledges support from the NSF MRSEC 'Micro- and Nano-mechanics of electronic and structural materials' at Brown University. WAC thanks Mr M Dewald for collaboration on the one-dimensional model calculations. RM also acknowledges support from the NSERC of Canada.

References

[1] Jarvis E A A, Hayes R L and Carter E A 2001 Effects of oxidation on the nanoscale mechanisms of crack formation in aluminum *Chem. Phys. Chem.* **2** 55–9

[2] Gall K, Horstemeyer M F, Van Schilfgaarde M and Baskes M I 2000 Atomistic simulations on the tensile debonding of an aluminum-silicon interface *J. Mech. Phys. Solids* **48** 2183–212

[3] Erik van der Giessen and Alan Needleman 1995 Discrete dislocation plasticity: a simple planar model *Modeling Simul. Mater. Sci. Eng.* **3** 689–735

[4] Cleveringa H H M, van der Giessen E and Needleman A 1997 Comparison of discrete dislocation and continuum plasticity predictions for a composite material *Acta Mater.* **45** 3163–79

[5] Kubin L P and Canova G 1992 The modelling of dislocation patterns *Scr. Meter.* **27** 957–62

[6] Radeke M R and Carter E A 1997 *Ab initio* derived kinetic monte carlo model of h_2 desorption from si(100)-2×1 *Phys. Rev.* B **55** 4649–58

[7] Gehlen P C, Hahn G T and Kanninen M F 1972 Crack extension by bond rupture in a model of bcc iron *Scr. Meter.* **6** 1087–90

[8] Gehlen P C 1973 Crack extension in a model of α-iron *Scr. Meter.* **7** 1115–18

[9] Sinclair J E 1975 The influence of the interatomic force law and of kinks on the propagation of brittle cracks *Phil. Mag.* **31** 647–71

[10] Baskes M I, Melius C F and Wilson W D 1981 *Interatomic Potentials and Crystalline Defects* ed J K Lee (New York: Metallurgical Society of AIME) pp 249–71

[11] Mullins M and Dokainish M A 1982 Simulation of the (001) plane crack in α-iron employing a new boundary scheme *Phil. Mag.* A **46** 771–87

[12] Mayes Mullins 1984 Atomic simulation of cracks under mixed mode loading *Int. J. Fracture* **24** 189–96

[13] Miller R E 2003 Direct coupling of atomistic and continuum mechanics in computational materials science *J. Multiscale Comput. Eng.* **1** 57

[14] Honglai Tan 2003 Combined atomistic and continuum simulation for fracture and corrosion *Comprehensive Structural Integrity: Interfacial and Nanoscale Failure* vol 8, ed W W Gerberich and W Yang (New York: Elsevier Science)
[15] Rodney D 2003 Mixed atomistic/continuum methods: static and dynamic quasicontinuum methods *Proc. NATO Conf. Thermodynamics, Microstructures and Plasticity* ed A Finel *et al* (Dortrecht: Kluwer) to appear
[16] Ortiz M and Phillips R 1999 Nanomechanics of defects in solids *Adv. Appl. Mech.* **36** 1–79
[17] Ortiz M, Cuitino A M, Knap J and Koslowski M 2001 Mixed atomistic continuum models of material behavior: the art of transcending atomistics and informing continua *MRS Bull.* **26** 216–21
[18] Abraham F F, Bernstein N, Broughton J Q and Hess D 2000 Dynamic fracture of silicon: concurrent simulation of quantum electrons, classical atoms, and the continuum solid *Mater. Res. Soc. Bull.* **25** 27–32
[19] Carlsson A E 1990 Beyond pair potentials in elemental transition metals and semiconductors *Solid State Phys.* **43** 1–91
[20] Hughes T J R 1987 *The Finite Element Method: Linear Static and Dynamic Finite Element Analysis* (Englewood Cliffs, NJ: Prentice-Hall)
[21] Zienkiewicz O C 1991 *The Finite Element Method* 4th edn, vol 1–2 (London: McGraw-Hill)
[22] Payne M C, Teter M P, Allan D C, Arias T A and Joannopoulos J D 1992 Iterative minimization techniques for ab initio total energy calculations: molecular dyanmics and conjugate gradients *Rev. Mod. Phys.* **64** 1045–97
[23] Broughton J Q, Abraham F F, Noam Bernstein and Efthimios Kaxiras 1999 Concurrent coupling of length scales: methodology and application *Phys. Rev.* B **60** 2391–403
[24] Daw M S and Baskes M I 1984 Embedded-atom method: derivation and application to impurities, surfaces, and other defects in metals *Phys. Rev.* B **29** 6443–53
[25] Norskøv J K and Lang N D 1980 Effective-medium theory of chemical binding: application to chemisorption *Phys. Rev.* B **21** 2131–6
[26] Stillinger F H and Weber T A 1985 Computer-simulation of local order in condensed phases of silicon *Phys. Rev.* B **31** 5262–71
[27] Payne M C, Robertson I J, Thomson D and Heine V 1996 *Ab initio* databases for fitting and testing interatomic potentials *Phil. Mag.* B **73** 191–9
[28] Yang L H, Soderlind P and Moriarty J A 2001 Accurate atomistic simulation of $(a/2)\langle 111\rangle$ screw dislocations and other defects in bcc tantalum *Phil. Mag.* A **81** 1355–85
[29] Baskes M I and Johnson R A 1994 Modified embedded atom potentials for hcp metals *Modeling Simul. Mater. Sci. Eng.* **2** 147–63
[30] Tersoff J 1988 Empirical interatomic potential for silicon with improved elastic properties *Phys. Rev.* B **38** 9902–5
[31] Brenner D W 1990 Empirical potential for hydrocarbons for use in simulating the chemical vapor deposition of diamond films *Phys. Rev.* B **42** 9458–71
[32] Pettifor D G, Oleinik I I, Nguyen-Manh D and Vitek V 2002 Bond-order potentials: bridging the electronic to atomistic modelling hierarchies *Computa. Mater. Sci.* **23** 33–7
[33] Pettifor D G and Oleinik I I 2002 Analytic bond-order potential for open and close-packed phases *Phys. Rev.* B **65** 172103
[34] Ericksen J L 1984 *Phase Transformations and Material Instabilities in Solids* ed M Gurtin (New York: Academic) pp 61–77
[35] Weiner J H 1983 *Statistical Mechanics of Elasticity* (New York: Wiley)
[36] Milstein F 1980 Review: theoretical elastic behavior at large strains *J. Mater. Sci.* **15** 1071–84
[37] Tadmor E B, Ortiz M and Phillips R 1996 Quasicontinuum analysis of defects in solids *Phil. Mag.* A **73** 1529–63
[38] Shenoy V B, Miller R, Tadmor E B, Phillips R and Ortiz M 1998 Quasicontinuum models of interfacial structure and deformation *Phys. Rev. Lett.* **80** 742–5
[39] Rudd R E and Broughton J Q 2000 Concurrent coupling of length scales in solid state systems *Phys. Status Solidi* b **217** 251–91
[40] Kohlhoff S, Gumbsch P and Fischmeister H F 1991 Crack propagation in bcc crystals studied with a combined finite-element and atomistic model *Phil. Mag.* A **64** 851–78
[41] Knap J and Ortiz M 2001 An analysis of the quasicontinuum method *J. Mech. Phys. Solids* **49** 1899–923
[42] Shilkrot L E, Miller R E and Curtin W A 2002 Coupled atomistic and discrete dislocation plasticity *Phys. Rev. Lett.* **89** 025501-1–025501-4
[43] Shenoy V B, Miller R, Tadmor E B, Rodney D, Phillips R and Ortiz M 1998 An adaptive methodology for atomic scale mechanics: the quasicontinuum method *J. Mech. Phys. Solids* **47** 611–42
[44] Miller R, Tadmor E B, Phillips R and Ortiz M 1998 Quasicontinuum simulation of fracture at the atomic scale *Modeling Simul. Mater. Sci. Eng.* **6** 607–38

[45] Miller R, Ortiz M, Phillips R, Shenoy V and Tadmor E B 1998 Quasicontinuum models of fracture and plasticity *Eng. Fracture Mech.* **61** 427–44
[46] Pillai A R and Miller R E 2001 Crack behaviour at bi-crystal interfaces: a mixed atomistic and continuum approach *Mater. Res. Soc. Symp. Proc.* **653** Z2.9.1–Z2.9.7
[47] Hai S and Tadmor E B 2003 Deformation twinning at aluminum crack tips *Acta Mater.* **51** 117
[48] Tadmor E B, Miller R, Phillips R and Ortiz M 1999 Nanoindentation and incipient plasticity *J. Mater. Res.* **14** 2233–50
[49] Picu P C 2000 Atomistic-continuum simulation of nano-indentation in molybdenum *J. Comput.-Aided Mater. Des.* **7** 77–87
[50] Shenoy V B, Phillips R and Tadmor E B 200 Nucleation of dislocations beneath a plane strain indenter *J. Mech. Phys. Solids* **48** 649–73
[51] Smith G S, Tadmor E B and Kaxiras E 2000 Multiscale simulation of loading and electrical resistance in silicon nanoindentation *Phys. Rev. Lett.* **84** 1260–3
[52] Smith G S, Tadmor E B, Bernstein N and Kaxiras E 2001 Multiscale simulations of silicon nanoindentation *Acta Mater.* **49** 4089–101
[53] Bernstein N and Kaxiras E 1997 Nonorthogonal tight-binding hamiltonians for defects and interfaces in silicon *Phys. Rev.* B **56** 10488–96
[54] Rodney D and Phillips R 1999 Structure and strength of dislocation junctions: an atomic level analysis *Phys. Rev. Lett.* **82** 1704–7
[55] Mortensen J J, Schiøtz J and Jacobsen K W 2002 The quasicontinuum method revisited *Challenges Mol. Simul.* **4** 119
[56] Shin C S, Fivel M C, Rodney D, Phillips R, Shenoy V B and Dupuy L 2001 Formation and strength of dislocation junctions in fcc metals: a study by dislocation dynamics and atomistic simulations *J. Phys.* IV **11** 19–26
[57] Phillips R, Rodney D, Shenoy V, Tadmor E B and Ortiz M 1999 Hierarchical models of plasticity: dislocation nucleation and interaction *Modeling Simul. Mater. Sci. Eng.* **7** 769–80
[58] Shenoy V, Shenoy V and Phillips R 1999 Finite temperature quasicontinuum methods *Mater. Res. Soc. Symp. Proc.* **538** 465–71
[59] Miller R E and Tadmor E B 2003 The quasicontinuum method: overview, applications and current directions *J. Comput.-Aided Mater. Des.* at press
[60] Tadmor E B, Smith G S, Bernstein N and Kaxiras E 1999 Mixed finite element and atomistic formulation for complex crystals *Phys. Rev.* B **59** 235–45
[61] Miller R E 1997 On the generalization of continuum models to include atomistic features *PhD Thesis* Brown University
[62] Shilkrot L E, Miller R E and Curtin W A 2003 Multiscale plasticity modelling: Coupled atomistics and discrete dislocation mechanics *J. Mech. Phys. Sol.* submitted
[63] Abraham F F, Broughton J Q, Bernstein N and Kaxiras E 1998 Spanning the length scales in dynamic simulation *Comput. Phys.* **12** 538
[64] Rudd R E 2001 Concurrent multiscale modeling of embedded nanomechanics *Mater. Res. Soc. Symp. Proc.* **677** AA1.6.1–AA1.6.12
[65] Wei Yang, Honglai Tan and Tianfu Guo 1994 Evolution of crack tip processes *Modeling Simul. Mater. Sci. Eng.* **2** 767–82
[66] Shilkrot L E, Curtin W A and Miller R E 2002 A coupled atomistic/continuum model of defects in solids *J. Mech. Phys. Solids* **50** 2085–106
[67] Rudd R E and Broughton J Q 1998 Coarse-grained molecular dynamics and the atomic limit of finite elements *Phys. Rev.* B **58** R5893–6
[68] Wei Cai, Maurice de Koning, Bulatov V V and Yip S 2000 Minimizing boundary reflections in coupled-domain simulations *Phys. Rev. Lett.* **85** 3213–16
[69] Weinan E and Zhongyi Huang 2001 Matching conditions in atomistic-continuum modeling of materials *Phys. Rev. Lett.* **87** 135501-1–135501-4
[70] LeSar R, Najafabadi R and Srolovitz D J 1989 Finite-temperature defect properties from free-energy minimization *Phys. Rev. Lett.* **63** 624–7
[71] Curtaloro S and Ceder G 2002 Dynamics of an inhomogeneously coarse grained multiscale system *Phys. Rev. Lett.* **88** 255504
[72] Peter Gumbsch and Glenn E Beltz 1995 On the continuum versus atomistic descriptions of dislocation nucleation and cleavage in nickel *Modeling Simul. Mater. Sci. Eng.* **3** 597–613
[73] Rudd R E and Broughton J Q 1999 Atomistic simulation of mems resonators through the coupling of length scales *J. Model. Simul. Microsyst.* **1** 29–38